Redistribution of recent collision push and ridge push in Central Europe: insights from FEM Modelling.

Jarosinski, M.; Beekman, W.W.W.; Bada, G.; Cloetingh, S.A.P.L.

published in
Geophysical Journal International
2006

DOI (link to publisher)
10.1111/j.1365-246X.2006.02979.x

document version
Publisher's PDF, also known as Version of record

Geophys. J. Int. (2006) **167,** 860–880 doi: 10.1111/j.1365-246X.2006.02979.x

Redistribution of recent collision push and ridge push in Central Europe: insights from FEM modelling

M. Jarosiński,[1] F. Beekman,[2] G. Bada[2,3] and S. Cloetingh[2]

[1]*Polish Geological Institute,* 00-975 *Warsaw, Rakowiecka str.* 4, *Poland. E-mail: marek.jarosinski@pgi.gov.pl*
[2]*Faculty of Earth and Life Sciences, Vrije Universiteit, Amsterdam, the Netherlands*
[3]*Department of Geophysics, Eötvös L. University, Budapest, Hungary*

Accepted 2006 February 21. Received 2006 February 21; in original form 2005 July 9

SUMMARY

2-D elastic finite element models of the recent stress field of Central Europe are built to evaluate the loads exerted on the continental boundary and the magnitude of tectonic stresses within the continental part of the plate. The models comprise 24 tectonic blocks (their stiffness is either constant throughout the model or varies from block to block), 16 fault zones and 12 geologically significant boundary segments. We have obtained a relatively unique balance of external tectonic forces by (1) careful adjustment of calculated stress directions and regimes to complex pattern of stress from data and (2) by calibration with gravitational potential energy. A high level of compression (*ca.* 9×10^{12} N m^{-1}) exerted to the short Ionian side of the Adriatic indenter is crucial for the stress-field pattern in Central Europe. The Adria microplate rotates due to eccentricity between the Africa push from the south and the Alpine buttress to the north. A free boundary of the Apennines does not contribute significantly to this motion. Kinematics of this indenter is controlled by friction on the Dinaric suture, which, in turn is decisive for strain-energy distribution between the Alpine and the Pannonian domains. The predicted pronounced extension in the Greece–Aegean segment (2.5×10^{12} N m^{-1}) implies active pull transferred from the Hellenic subduction zone. This extension releases stress in the Balkan–Pannonian region and enables the eastward escape of tectonic blocks in front of advancing Adria. Significant changes of tectonic push trends are found along the Black Sea–Caucasus boundary segment and at the European passive margin from the North Sea to the Arctic Ocean. Differential stresses in Central Europe are estimated in the range of 10–60 MPa when averaged over the 30–80-km-thick mechanically heterogeneous lithosphere. The maximum stiffness contrast across the model is predicted to be of one order of magnitude. Apparent friction coefficients of fault zones differ between the North European part of the plate (0.4–0.7), the Pannonian region (0.15–0.25) and the Dinaric suture (0.55).

Key words: finite element method, geodynamics, stresses distribution, tectonics.

1 INTRODUCTION

In this paper we evaluate the variation of recent tectonic forces and stresses acting in the Central European portion of continental Eurasia. A prominent feature of the examined area is the high heterogeneity of the recent stress field in terms of maximum horizontal stress (S_{Hmax}) direction and stress regime conditions. In a vast area comprising the East European Craton (EEC), the Alps, the Carpathians and parts of the Pannonian–Dinaric region, the S_{Hmax} deviate significantly from the general NW–SE trend that is characteristic for Western Europe and Fennoscandia (Müller *et al.* 1992). We investigate whether external tectonic forces supplemented by topography-related stresses can produce the observed complex stress pattern in the plate interior. Of special interest are magnitudes of forces and ratios between forces, acting on separate segments of the Eastern Mediterranean-Caucasus collision zone. Also the consequences of ridge push variations along the NW European passive margin for the stress-field variability in Europe are explored. To date, plate-scale models were structurally too simple to account for these more detailed phenomena. By constructing of successively more complex models we test the possible influence of singular factors like topographic stresses, active faults or stiffness differentiation of tectonic blocks on redistribution of external loads within intracontinental environment of Central Europe.

Besides the main issues of forces and stresses we also addressed the kinematics of tectonic blocks. A vital point is kinematics of the Adriatic microplate (Adria) and its geodynamic position in a collisional context. On one hand, Adria is proposed to represent the African promontory, what implies a mechanical coupling between these two plates (Channell *et al.* 1979; Mantovani *et al.* 1990).

Alternatively, the independent rotation of Adria, due to opening of the Tyrrhenian Sea, is proposed by Dercourt *et al.* (1986) and Locardi (1988). Although recent space geodesy measurements indicate a kinematic independence of Adria from Africa (e.g. Ward 1994), the tectonic force balance and its control on the Adria motion are still unresolved.

The results of our modelling highlight some other specific problems concerning the still questioned geodynamics of tectonic blocks in Central Europe. For instance, it is proposed that ongoing extrusion of blocks from the Southern and Eastern Alps towards the Pannonian basin (Grenerczy *et al.* 2000; Peresson & Decker 1997) is driven by the potential energy gradient between the Alpine orogen and the Pannonian basin (Bada *et al.* 2001). The other plausible mechanism is the squeezing out of these blocks due to tectonic push of the Adria indenter. This alternative is tested by the implementation of topography-related stresses and by incorporating faults that enable escape of tectonic blocks. Some earlier published numerical models have emphasized the importance of the Vrancea push for the stress field in the Pannonian region (Grünthal & Stromeyer 1992; Bada *et al.* 1998). However, due to a break-off stage of sinking slab in Vrancea (Wortel & Spakman 2000; Cloetingh *et al.* 2004), sinking of the detached plate without significant impact on regional horizontal stress is also likely. Our research presented in this paper verifies whether any additional horizontal tectonic force in the Vrancea and another intracontinental realm is necessary, or whether external forces alone are sufficient to explain the overall stress distribution in Central Europe.

1.1 Previous elastic finite element models of Central Europe

The present-day intraplate stress field of Europe has frequently been the object of a numerical elastic finite element modelling (Table 1). The earliest model presented by Grünthal & Stromeyer (1992) constructed with a coarse mesh ($2^\circ \times 2^\circ$), simplified geometry and lacked faults and topography-related stresses. The best prediction of stress direction was obtained for a low stiffness differentiation between tectonic units. The authors concluded that the Young's modulus and boundary forces could be scaled up and down by the same factor, without a visible effect on the modelled stress field. One of the possible reasons of such behaviour is the extreme tightness of the model, expressed by absence of extension and high ratio of horizontal compressive stresses ($S_h/S_H > 0.6$). The calculated orientation of S_H substantially differs from a set of observations for the Dinarides, the Pannonian basin and the edge of the EEC (Reinecker *et al.* 2003). This discrepancy (Grünthal & Stromeyer 1992) supported the presence of ongoing subduction in the Carpathians, the importance of the Vrancea push and active extension in the Pannonian basin.

In the elastic FEM model of the European plate by Gölke & Coblentz (1996), ridge push was simulated in two ways, as a line force exerted to the plate boundary or as a distributed body force, integrated over the oceanic plate. As a result, the magnitude of forces due to the Atlantic ridge push was estimated to be two to three $\times 10^{12}$ N m^{-1}. For the north European continental margin these forces produce intraplate stresses in the range of 10–20 MPa (averaged over a 100-km-thick lithosphere). The collision forces of Africa with Eurasia were estimated at 0.5×10^{12} N m^{-1} in the western Mediterranean segment, and 2.0×10^{12}N m^{-1} in the eastern one. However, the misfit between the calculated S_H and observed S_{Hmax} directions is substantial, in places where the data show significant deviations from a steady NW–SE trend (we use symbols S_H and S_{Hmax} for the modelled maximum horizontal stress and for the stress data, respectively).

Bada (1999) constructed more local scale models, limited to the Pannonian region, with boundary loads applied to the surrounding mountain ranges. He incorporated a variable tectonic block stiffness and active faults in one set of models and topography-related stresses in the second set (Bada *et al.* 2001). The first-order stress pattern was satisfactorily predicted, permitting identification of several factors

Table 1. Comparison of FEM elastic models of contemporary stress field for Europe.

Model references	Geographical range	Elements	Coordinate system	Mechanical property diff.	Boundary conditions	Topographical stress faults
Grünthal & Stromeyer (1992)	Europe, plate-scale, focused on Central Europe	Elastic membrane shell coarse >200 km	Plane stress	Non-uniform E: 40–100 GPa $\nu = 0.3$	Pressure—normal to plate/ model boundary	No topography, no faults
Gölke & Coblentz (1996)	European part of Eurasia—plate-scale model	Triangular, shell 100 km	Cartesian	Uniform $E = 70$ GPa $\nu = 0.25$	Ridge push—body force or linear 0 net torque	Topography no faults
Bada (1999)	Pannonian region, Alps, Carpathians,	Quadratic, 50 km	Cartesian	Nonuniform E: 40–100 GPa $\nu = 0.25$	Displacements no basal drag	No topography faults as contacts
Bada *et al.* (2001)	Pannonian region, Alps & Carpathians,	Shell 50 km	Spherical	Nonuniform E: 40–100 GPa $\nu = 0.25$	Boundary fixed or displacements	Topography no faults
Loohuis *et al.* (2001)	Eurasian plate	Shell	Spherical	Uniform $E = 70$ GPa $\nu = 0.25$	Ridge push—body force basal drag 0 net torque	Topography no faults
Mantovani *et al.* (2000)	East Mediterranean Apennine & Balkans	Plane stress triangle element >100 km	Cartesian	Non-uniform $10^{10} < M^* < 10^{16}$ $\nu = 0.25$	Displacements no basal drag	No topography faults as elastic anisotropy
Andeweg (2001)	European part of Eurasia, focused on Iberia	100 km	Spherical	Uniform	Ridge push as a body force, no basal drag	Topography no faults
Jarosiński, this paper	Central Europe, Scandinavia & Balkans	Triangular with mid nodes, 25–50 km	Carthesian	Non-uniform E: 40–100 GPa $\nu = 0.25$	Pressures and forces no basal drag	Topography faults thickness

$^*M = E \times Th$—stiffness parameter, expressed by Young modulus (E) and lithospheric thickness (Th) respectively.

responsible for recent geodynamics of the Pannonian region. They are: rotation of Adria, Vrancea push, the Bohemian massif buttressing effect and topographic stresses. Topographic stresses, although significant in the elevated areas, appear to have minor impact on the stress field in surrounding lowlands.

Goes *et al.* (2000) presented a model for the whole Eurasian plate with implemented basal drag in direction of absolute plate motion and the boundary forces in direction of relative plate motions. The zero net torque condition allows for an evaluation of resistive drag forces. They obtained a relatively low average magnitude of Eurasia/Africa collision force of 1×10^{12} N m^{-1}, which resulted from incorporation of basal drag. However, the calculated stress directions mismatch both the local trends and the regional trend characteristic for Western Europe. Based on these results, Goes *et al.* (2000) arrived at the conclusion that a simple balance between ridge push and collision forces cannot explain the stress pattern in Europe, but that thermal anomalies in the upper mantle in the order of 300°C have to be considered when modelling the regional intraplate stresses.

Mantovani *et al.* (2000) showed that the recent strain rate field of the eastern Mediterranean can be reproduced by a 2-D elastic plate FEM model of the Africa–Eurasia collision zone. This was possible by assigning a highly differential rigidity and elastic anisotropy for different tectonic units. The calculated field of deformation was comparable to the measured geodetic strain (McClusky *et al.* 2000), except for the Hellenic arc where measured strains are considerably higher than modelled. Although this active subduction zone could not be fully reproduced in a 2-D model, the authors concluded that a slab pull does not notably influence the recent deformation field in the Mediterranean region.

Andeweg (2002) presented an elastic FEM model of the Iberia peninsula and also the most general model for Europe, which was used to verify three different methods of distributed ridge push calculations. Except for Scandinavia and the Balkan area, different approaches resulted in similar distribution of differential stresses for the entire Central European area in the range of 0–20 MPa (averaged over 100 km lithosphere), which is comparable with stresses predicted by Gölke & Coblentz (1996).

1.2 FEM model integrating faults and topography-related stresses

The modelling approach presented in this paper is closest to the approach by Bada *et al.* (1998, 2001). However, in comparison to their model, the present one is extended geographically to the borders of continental Europe, which enables to apply the boundary loads at far-field distance from the Carpathian–Pannonian region. The distant boundaries and the complex internal geometry allow an intricate interplay between several intracontinental lithospheric blocks, some of which are separated by faults. Moreover, the orientation and magnitude of the intraplate stresses generated by the applied far-field boundary forces may change substantially and/or abruptly across the boundaries of the intracontinental blocks. Another step forward is the incorporation of gravitational potential energy and faults in a single model.

Due to its specific arrangement, the presented model addresses different questions from those posed in previous publications. Combining in one model topographic stresses, fault behaviour and stress regimes permits to obtain independent constraints of boundary forces and stress magnitudes. Using different material properties for tectonic units and faults as variable model parameters enable us to find the maximum rheological contrast across the model. Generally, the presented approach contributes to bridge the gap between plate-scale models, which often have a poor fit between predicted and observed stress data and local-scale models, which typically suffer from a too tight relation between the loads and stresses.

2 RECENT GEODYNAMIC FRAMEWORK

The modelled area is limited to the central and eastern European part of continental Eurasia (Fig. 1). The region comprises a complex structural junction, divided by the Alpine–Carpathian suture into the North European foreland part of the plate, and the South European hinterland part of the plate. The North European plate embraces the EEC and the Palaeozoic platform, consisting of Avalonia and Armorica terranes accreted to Baltica in the Caledonian and Variscan times, respectively (Ziegler 1982). The South European plate comprises an array of terranes amalgamated to the North European plate in Tertiary during the Alpine collision.

2.1 North European plate

The eastern section of the model is occupied by the EEC, which constitutes the most stable part of Europe. Due to its northern position the Fennoscandian part of the EEC is preferentially exposed to the Atlantic ridge push, which produces horizontal stresses (S_{Hmax}) perpendicular to the continental margin (Fig. 2). The present-day geodynamics of Fennoscandia is also affected by post-glacial isostatic rebound and by extension of the continental margin (Fejerskov & Lindholm 2000). From focal mechanism solutions (Stephansson *et al.* 1991) and structural observations (Pascal *et al.* 2005) supporting compressive stress regimes, both strike-slip and thrust fault, are well constrained for this region. GPS measurements demonstrate radial horizontal extension of Fennoscandia around the Gulf of Bothnia at the rate >1 mm yr^{-1} (Milne *et al.* 2001). In the vicinity of this gulf, which is the centre of post-glacial isostaic uplift, S_{Hmax} directions deviate from the general NW–SE trend. Within the interior of the EEC single good-quality stress determination from borehole breakouts indicates NW–SE direction of S_{Hmax} in the crystalline basement (Huber *et al.* 1997). The edge of the EEC in Poland is dominated by a stable N–S-oriented compression (Jarosiński 2005a).

The EEC is separated from the Palaeozoic platform by the Teisseyre-Tornquist zone (TTZ) extending from the North Sea to the Black Sea. Breakout measurements from the Polish segment of the TTZ show a S_{Hmax} rotation with depth and a distortion in plane ranging from N–S to NW–SE (Jarosiński 1999, 2005a). In spite of the fact that stress perturbations like these favour strike-slip reactivation, only minor seismicity is reported from the central segment of the TTZ (Guterch & Lewandowska-Marciniak 1975; Gibowicz *et al.* 1981). GPS measurements in the northern segment, called the Sorgenfrei-Tornquist zone (STZ), show a transtensional strike-slip offset with the rate of 2 mm yr^{-1} (Pan *et al.* 2001). Also intensive seismicity in Scåne points to recent tectonic reactivation of the STZ (Wahlstrom & Grunthal 1994).

The Palaeozoic platform comprises a mosaic of tectonic massifs like Elbe, Black Forest, Ardens, Bohemian and Bruno-Vistulicum. These blocks form relatively rigid inclusions characterized by lower surface heat flow (Hurtig *et al.* 1992). They are separated mainly by NW–SE trending, transcrustal fault zones like the Frankonian line, the Danube Fault, the Elbe-Hamburg line or the Odra Fault (Ziegler 1982), active during the late Variscan strike-slip event (Arthoud & Matte 1977; Aleksandrowski 1995; Matte 1991). There are also

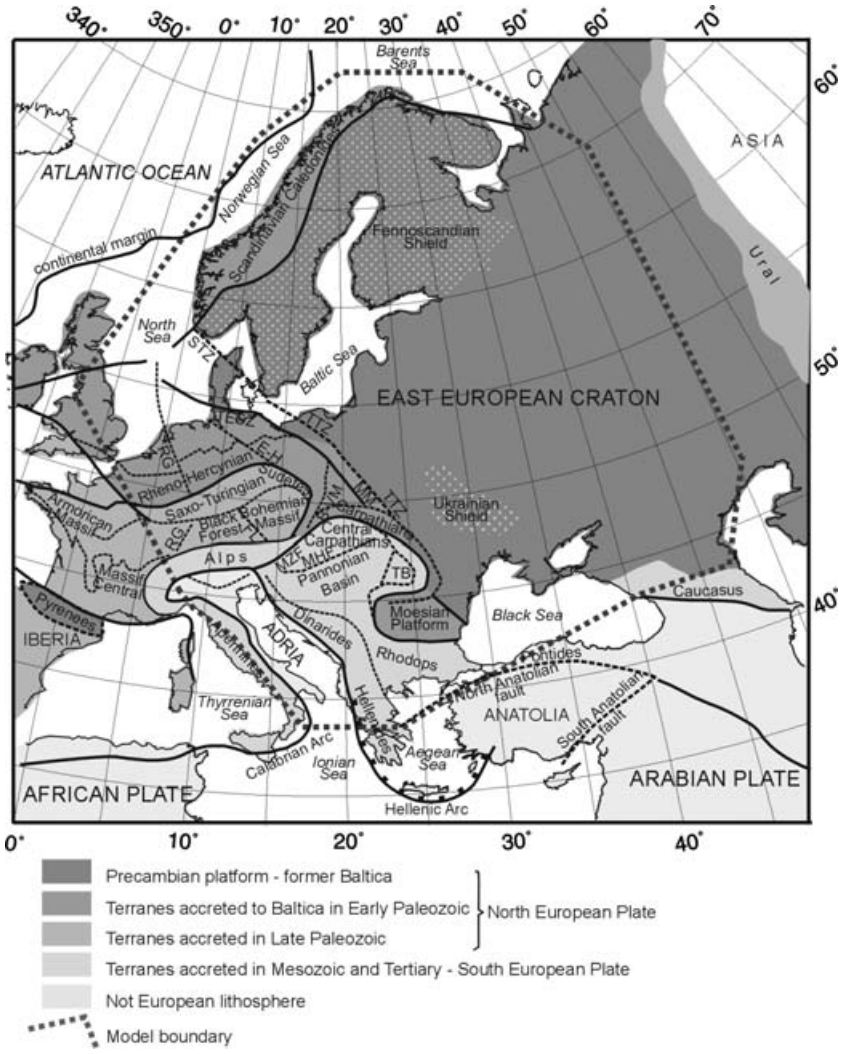

Figure 1. Location of the model area (thick dashed line) over the background of the tectonic sketch of Europe, after Berthelsen (1992), modified. B-VM—Bruno-Vistulicum massif; H-E—Hamburg-Elba fault zone; MHF—mid-Hungarian fault zone; MM—Małopolska massif; MZF—Mur-Žilina fault zone; RG—Rhine graben; STZ—Sorgenfrei-Tornquist fault zone; TB—Transylvanian basin; TESZ—Trans-European suture zone; TTZ—Teisseyre-Tornquist fault zone.

some N–S or NE–SW trending structures, like the Rhine graben, the Eger graben and the Moravo-Silesian zone (Ziegler & Cloetingh 2004). For this western part of Europe a relatively constant NW–SE mean direction of S_{Hmax} is representative. However, significant and sometime systematic regional deviations from this trend suggest quite complex interactions between tectonic blocks. For instance, in northwestern Poland and northeastern Germany S_{Hmax} takes a different NNE–SSW direction (Roth & Fleckenstein 2001; Jarosiński 2005a) (Fig. 2). A strike-slip stress regime prevails in the Palaeozoic platform of Western Europe (Müller *et al.* 1997). The southern end of the North European plate sinks below the Alpine and the Carpathian accretionary wedges and foredeep basins. Thin-skinned tectonic push from the Alps is assumed to be responsible for stress partitioning in the eastern part of the Alpine Molasse basin, where the S_{Hmax} direction changes from NW–SE, below a décollement along Triassic evaporates, to N–S or NNE–SSW above them (Brereton & Mueller 1991). A similar stress partitioning was inferred for the western segment of the Polish Carpathians, where the NNE–SSW-oriented S_{Hmax} in the accretionary wedge differs significantly from the NNW–SSE direction in the autochthonous basement (Jarosiński 1998). In the eastern segment of the Polish Carpathians, S_{Hmax} direction varying between NNE–SSW and ENE–WSW (Jarosiński 1998, 2005a) parallels the Carpathian push derived from GPS measurements (Hefty 1998).

The Carpathian suture was finally shaped in the course of slab detachment from the continental part of the North European plate (Matenco *et al.* 1997; Nemcok *et al.* 1998; Wortel & Spakman 2000). The break-off has been proceeding since the Late Miocene and is presently in the final stage in the Vrancea region (Oncescu 1987). Focal mechanism solutions of shallow earthquakes (depth <70 km) show that the foreland plate before the Vrancea orogenic corner is being subjected to radial S_{Hmax}, perpendicular to the orogenic arc, with a relative balance between three types of stress regimes (Radulian *et al.* 2000; Reinecker *et al.* 2003). The Southern Carpathians are characterized by the S_{Hmax} striking along the orogen in W–E direction and by dominance of strike-slip and extensional stress regimes. In Dobrogea, a WNW–ESE orientation of S_{Hmax} and a normal fault stress regime prevails, although also sinistral strike-slip motions along NW-striking planes are inferred from earthquake focal mechanisms (Radulian *et al.* 2000).

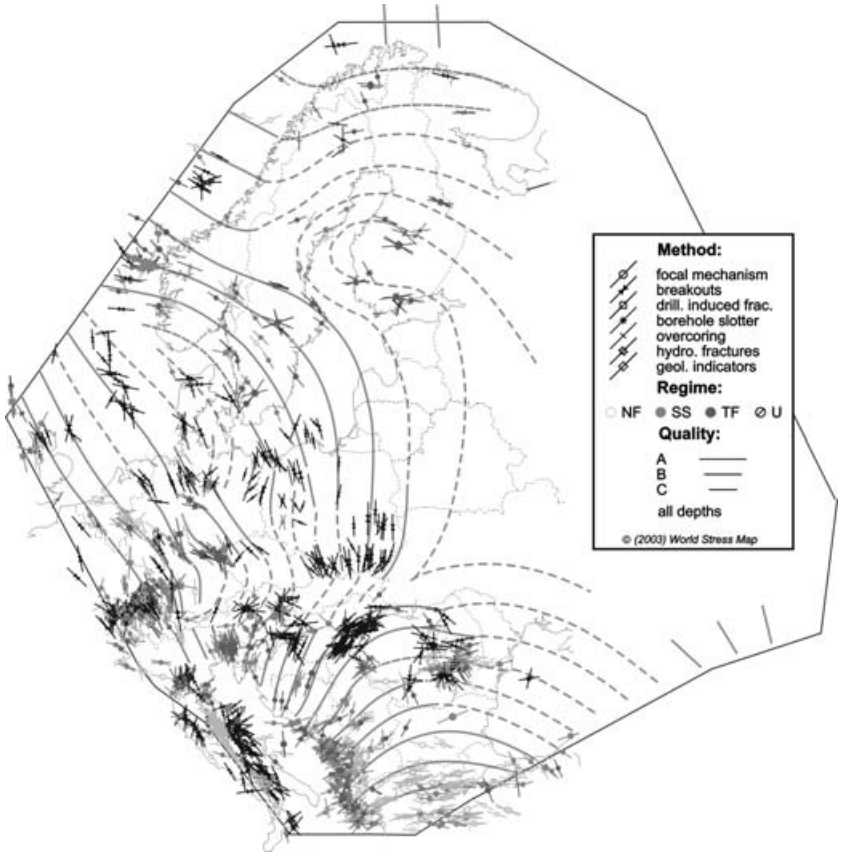

Figure 2. Recent stress field of Central Europe based on the World Stress Map database (Reinecker *et al.* 2003) supplemented with the data in Roth & Fleckenstein (2001) and Jarosiński (2005a). Interpretative S_{Hmax} trajectories in grey: solid line—well constrained; dashed line—suspected, where data is lacking or inconsistent S_{Hmax} directions. NF- normal fault stress regime; SS—strike-slip stress regime; TF—thrust fault stress regime; U—unknown stress regime.

2.2 South European plate

The suture between the north and south European part of Eurasia passes through the Alps, and extends in the Carpathians along the Mur-Žilina fault zone and the Pieniny Klippen Belt. According to seismological studies, the Mur-Žilina fault zone shows recent strike-slip sinistral activity (Aric 1981; Gutdeutsch & Aric 1988; Gerner *et al.* 1999). The Carpathian–Pannonian part of the plate comprises the Alcapa, Tisza and Dacia tectonic blocks (Csontos 1995; Balla 1988; Fodor *et al.* 1999). The Pannonian basin subsided during the Neogene back arc extension and then, since the latest Pliocene until present, has been under compression (Horváth & Cloetingh 1996; Horváth 1995; Gerner *et al.* 1999). A complex pattern of S_{Hmax} is dominated by NE-oriented compression, in the transition from the Dinarides to the Pannonian basin, which turns towards W–E compression within the Tisza block. Here, large differential stresses up to 140 MPa have been inferred for a depth of 3 km (Gerner *et al.* 1999).

The Dinarides represent the suture between the Adria microplate and the Vardar units (Tari 2002). High seismicity in the Dinarides and their hinterland indicates intensive present-day deformations (Anderson & Jackson 1987; Console *et al.* 1993). The stress regimes change from more compressive in the northwestern Dinarides and the Southern Alps, where thrust fault stress regime prevails, through a mixed compressive/extensional regime in the southern Dinarides, to more extensional in the Helenides (Ward 1994). S_{Hmax} directions vary from NNE–SSW in the Dinaric/Alps junction to NE–SW in the southeastern Dinarides. In the Dinaric region seismic energy release is several orders of magnitude higher than in any other part of the Balkans and the Pannonian region (Gerner *et al.* 1999). It appears that a large part of the Adria push is discharged in this area. Within the Dinarides and their foreland, NW–SE trending dextral strike-slip faults partially accommodate the recent push of the Adriatic block (Gerner *et al.* 1999; Picha 2002).

In the Eastern Alps a fairly scattered S_{Hmax} pattern suggests small differential stress (Reinecker & Lenhardt 1999). GPS data show that the overall rate of convergence between Adria and the Bohemian massif in NNE–SSW direction reaches 8 ppb yr^{-1}, while across the Alps, contraction in N–S direction reaches 3 ppb yr^{-1} (Grenerczy *et al.* 2000). The Periadriatic line reveals dextral strike-slip motion at the rate of over 2 cm yr^{-1} (van Mierlo *et al.* 1997). Locally, some amount of extension within the Alpine orogen is also plausible (Champagnac *et al.* 2004).

The recent counter-clockwise rotation of the Adriatic microplate is recorded by GPS measurements (Jackson & McKenzie 1988). Stress regimes are not well constrained for the interior of the Adriatic block, since this rigid block reveals low seismicity (Chiarabba *et al.* 2005). Scarce earthquake focal mechanisms point to a mixed stress regime with dominance of strike-slip over the thrust fault regime (Anderson & Jackson 1987). A relatively high energy release in the Dalmacian part of the Adriatic suture and a relatively low energy release in the northern part (Gerner *et al.* 1999) correspond to the results of GPS measurements that indicate a moderate NW-directed intraplate motion of the northern segment of Adria (3–4 mm yr^{-1})

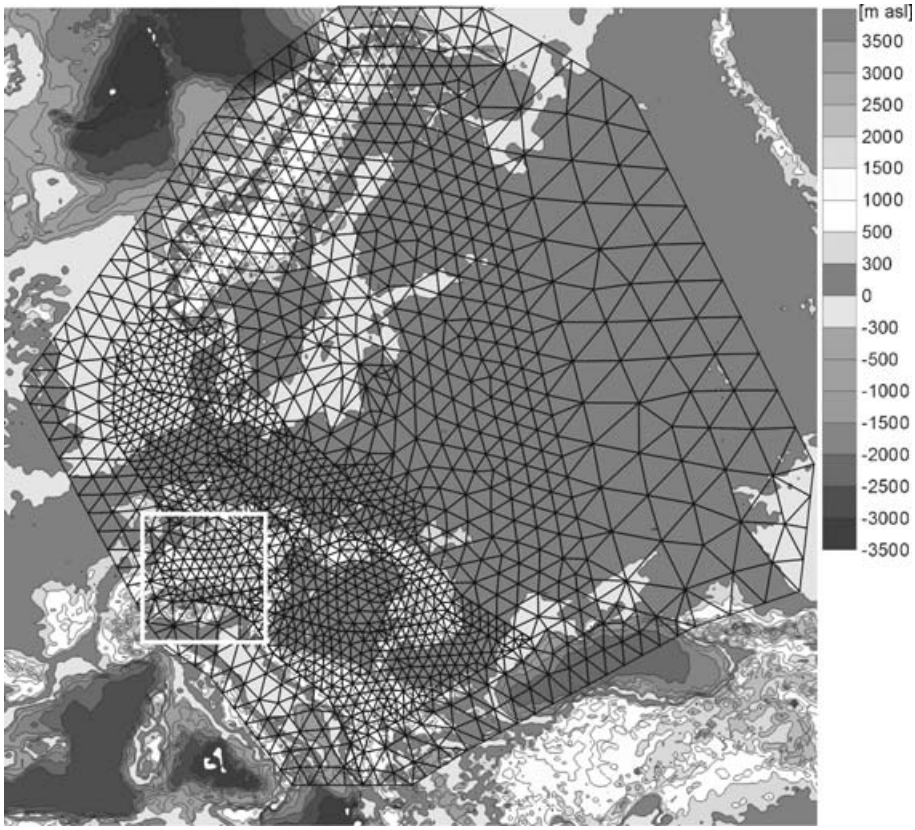

Figure 3. Model mesh over the background of a digital elevation model of Europe. Correction due to isostatically balanced topography was implemented for elevations or depressions exceeding ±300 m a.s.l./b.s.l. White square indicates location of Fig. 5.

(Grenerczy *et al.* 2000) and a faster northward motion of the central segment (10 mm yr^{-1}) (Altiner 2001).

The northward advance of the African plate and its tendency to counter-clockwise rotation dominates the overall collisional setting of Africa with Eurasia. The velocity of the convergence with Europe increases eastwards, from 6 mm yr^{-1} in the western part of Mediterranean to 9 mm yr^{-1} in the eastern part (Minster & Jordan 1978). The convergence of the Arabian plate is estimated to be more than 18 mm yr^{-1} (McClusky *et al.* 2000). A high rate of the Arabia push results in the westward extrusion of the Anatolian block at the rate of 20–24 mm yr^{-1} (Reilinger *et al.* 1997). Farther to the west, space geodesy shows that the Aegean stress province is characterized by a N–S and NNE–SSW oriented extension, which extends northwards to the Moesian Platform (Kahle *et al.* 2000). However, stress data indicate also the presence of a compressive stress regime in the Rhodope (Ward 1994; Reinecker *et al.* 2003). A GPS-derived kinematic model indicates a SSW-directed intraplate motion of the Aegean Sea at a rate 20–35 mm yr^{-1} (McClusky *et al.* 2000) that may be driven by the slab retreat in the active Hellenic subduction zone (Jolivet 2001). The convergence between Arabia and Eurasia is accommodated not only by the escape of Anatolia but also by shortening across the Caucasus at a rate of 12 mm yr^{-1} (Reilinger *et al.* 1997; McClusky *et al.* 2000).

3 SET UP OF THE MODEL

3.1 Structure of the model

The model comprises 3963 triangular, plane strain and stress solid elements with mid-nodes (Fig. 3). In the most detailed part of the model, the nominal size of the element side is 50 km, while in the peripheral areas a coarse mesh with 100–200 km element's size is constructed. The elements have elastic and isotropic strain and stress capabilities with constant Poisson's ratio and variable Young's modulus and thickness. The model incorporates also contact elements that simulate regional fault zones (Cook *et al.* 1989). Calculated compressive stresses are taken as positive and tensional stresses are negative. In compressive stress regimes both strike-slip and thrust fault can appear.

While building the model we took into consideration the following points.

(1) The model should be roughly symmetrical in relation to the axis of symmetry of the fixed eastern boundary to avoid major imbalance between force momentum attributed to the Atlantic ridge push on one side and to the Africa/Arabia push on the other side. It helps to minimize the net torque acting on the plate and thus minimizing the need to appeal to such devices as basal drag to ensure mechanical equilibrium.

(2) To enable comparison between different cases of tectonic load, the boundaries of the model were located approximately at zero sea level, which is also the reference level for the gravitational potential energy correction. Exceptions are the Ionian Sea, the eastern Black Sea segments and the cross-pass through the Alps (Fig. 3).

(3) To allow for fast changes of boundary loads the model boundaries were chosen to run parallel or perpendicular to the axes of local S_{Hmax} (Fig. 2).

A major mechanical contrast is expected across Central Europe due to the highly heterogeneous lithosphere and to large differences in surface heat flux. For example, the complex tectonic

Table 2. Tectono-mechanical units and their material properties.

Tectonic Unit		All models		Mod1-Mod5 No mechanical contrast		Mod6 & Mod7 Low mechanical contrast			Mod8 Extreme mechanical contrast		
		Heatflow [mW m^{-2}]	Poiss. ratio	E [MPa]	Th [km]	E^* [MPa]	Th^* [km]	Sf^* [$\times 10^{14}$]	E [GPa]	Th [km]	Sf [mPa] $\times 10^{14}$
TU1	EEC	40	0.25	70	100	**80**	**80**	**64**	**90**	**100**	**90**
TU2	LB	50	0.25	70	100	80	70	56	70	80	56
TU3	TF	60	0.25	70	100	80	70	56	80	80	64
TU4	TTZ	60	0.25	70	100	60	60	36	60	60	36
TU5	M-D	50	0.25	70	100	70	70	49	70	80	56
TU6	NGB	60	0.25	70	100	70	60	42	70	60	42
TU7	TESZ-N	70	0.25	70	100	60	40	24	50	30	15
TU8	TESZ-S	60	0.25	70	100	70	60	42	70	60	42
TU9	B-V	60	0.25	70	100	70	50	35	70	40	28
TU10	Sudetes	60	0.25	70	100	70	60	42	70	60	42
TU11	LSB	70	0.25	70	100	60	50	30	60	40	24
TU12	H-EM	50	0.25	70	100	70	70	49	70	70	49
TU13	E-F	80	0.25	70	100	60	40	24	50	30	15
TU14	BM	50	0.25	70	100	70	70	49	80	80	64
TU15	E Alps	70	0.25	70	100	60	50	30	60	40	24
TU16	TW+RW	70	0.25	70	100	60	50	30	60	40	24
TU17	ALCAPA	70	0.25	70	100	60	50	30	60	40	24
TU18	Tisza	90	0.25	70	100	**50**	**30**	**15**	**50**	**20**	**10**
TU19	TB	60	0.25	70	100	70	60	42	70	50	35
TU20	MP	50	0.25	70	100	80	70	56	80	90	72
TU21	Rhodop	60	0.25	70	100	70	60	42	70	60	42
TU22	Vardar—DH	80	0.25	70	100	50	40	20	50	30	15
TU23	Dinarides	60	0.25	70	100	70	60	42	70	50	35
TU24	Adria	–	0.25	70	100	70	100	70	70	100	70

Used symbols: E—Young's modulus, Th—lithosphere thickness, Sf—stiffness.
Tectonic Units: BM—Bohemian massif, DH—Dinaric hinterland, E Alps—Eastern Alps, EEC-East European craton, E-F—Eger graben-Franconian platform, H-EM—Harz-Erzgebirge massif, LB—Lublin basin, LSB—Lower Saxony basin, M-D—Moldavia—Dobrogea zone, MP—Moesian platform, NGB—North German basin, TF—Tornquist Fan, TB—Transylvanian basin, TESZ-N—Trans European suture zone—North segment, TTZ—Teisseyre-Tornquist zone, TW+RW—Tauern Window and Rechnitz Window.
Parameters: Sf—stiffness factor.

structure across the TTZ with a Moho depth changing from 30 to 45 km (Guterch *et al.* 1994, 1999) and heat flow variations from 80 mW m^{-2} to 40 mW m^{-2} (Majorowicz & Plewa 1979; Hurtig *et al.* 1992) gives rise to pronounced rheological contrasts (Jarosiński *et al.* 2002). A similar contrast is predicted between the Pannonian basin, having a 26-km-thick crust and a surface heat flow in the range of 70–100 mW m^{-2}, and the centre of the Bohemian massif with a more than 35-km-thick crust and a heat flow 50–60 mW m^{-2} (Lankreijer *et al.* 1999).

To account for mechanical heterogeneity of the continental lithosphere the main tectono-mechanical units (TU) were differentiated (Table 2). Within each unit material properties are assumed to be steady and are defined by: (1) Poisson's ratio $\nu = 0.25$ (constant throughout the model) and (2) Young's modulus (E) and elastic thickness (Th) (both can vary from unit to unit). Following the approach by Mantovani *et al.* (2000), the stiffness of each unit is expressed by the coefficient $Sf = E \times Th$ (Table 2). In this modelling study the material properties were modified in a wide range of values to find the maximum stiffness contrast, which may give a satisfactory model solution. Mechanical properties treated as model variables did not require a precise rheological constraints, but were instead estimated to the first order from published strength envelopes (Cloetingh & Banda 1992; Viti *et al.* 1997; Lankreijer *et al.* 1999; Jarosiński *et al.* 2002; Jarosiński & Da$_c$ browski 2006) and surface heat flow data (Hurtig *et al.* 1992). The approximated thickness of the elastic lithosphere was taken as a sum of thickness of the elastic cores of rheologically strong layers, taking into account differential stresses derived from preliminary models with constant material properties (models M3 in Chapter 5) . The Young's modulus (E) was approximated as the mean for lithological components of the elastic core: 40 GPa for sedimentary strata, 50 GPa for a granitic upper crust, 70–80 GPa for diorite or gabbro lower crust, and 90–100 GPa for the upper mantle (Turcotte & Schubert 1982). In order to obtain comparable boundary loads $E = 70$ GPa and thickness of 100 km were prescribed for units at the model boundary.

The FEM model of Europe includes sixteen regional-scale faults (Table 3). Each fault is built of several straight linear segments, which in turn contain several contact elements. The contact elements accommodate only planar strike-slip offset, which is an acceptable simplification for Central European domain where a strike-slip stress regime dominates (Müller *et al.* 1997; Jarosiński 2005b). Mechanical properties of faults are defined by a friction coefficient, which is constant for each fault segment. Introducing several major fault zones allows for inferences of the critical friction coefficient that prevents reactivation of passive faults or permits motion along recently active ones. Displacements along faults are accommodated largely by elastic deformation of the intracontinental blocks within the model continua and as a result the predicted fault offsets are relatively small and negligible when compared to the real tectonic fault displacement, accumulated over geological times. The predicted fault displacements are in the order of tens to hundreds of

Table 3. Fault zones and their apparent friction coefficients (μ_A).

	Fault zones	Mod1*	Mod2*	Mod3	Mod4	Mod5	Mod6	**Mod7**	Mod8
FZ1	Sorgenfrei-Tornquist	0.6	0.4	0.3	0.2	0.45	0.4	**0.4**	0.4
FZ2	Teisseyre-Tornquist	0.4	0.4	0.3	0.2	0.4	0.4	**0.4**	0.4
FZ3	Holy Cross-Dobrogea	0.6	0.4	0.3	0.2	0.45	0.4	**0.4**	0.4
FZ4	Trans-Europe Suture	0.6	0.5	0.3	0.2	0.45	0.4	**0.4**	0.4
FZ5	Sudetic-Moravian	0.6	0.4	0.3	0.2	0.45	0.4	**0.4**	0.4
FZ6	Kraków-Lubliniec	0.6	0.4	0.3	0.2	0.45	0.4	**0.4**	0.4
FZ7	Hamburg-Elba	0.8	0.6	0.3	0.2	0.45	0.5	**>0.5**	>0.5
FZ8	Franconian line	0.8	0.7	0.5	0.3	0.6	0.6	**>0.6**	>0.6
FZ9	Bavarian-Danube	0.8	0.6	0.3	0.2	0.45	0.4.	**0.4**	0.4
FZ10	Rhine graben	0.7	0.6	0.3	0.2	0.45	0.4	**0.4**	0.4
FZ11	Salzach-Ennstal	0.4	0.4	0.15	0.1	0.2	0.1	**0.15**	0.2
FZ12	Mur-Žilina+Lavanttal	0.6	0.4	0.15	0.1	0.2	0.1	**0.15**	0.2
FZ13	Pieniny Klippen Belt	0.4	0.4	0.35	0.2	0.6	0.4	**0.4**	0.5
FZ14	Mid-Hungarian	0.6	0.6	0.2	0.2	0.4	0.2	**0.25**	0.3
FZ15	Periadriatic–Drava	0.6	0.6	0.2	0.2	0.4	0.2	**0.25**	0.3
FZ16	Dinaride suture	1	1	0.55	0.4	0.65	0.5	**0.55**	0.6

*For Mod1 and Mod2 given are friction coefficients necessary to lock all faults.

metres, which appear to be sufficient to cause a remarkable local reorientation of the intraplate stresses.

3.2 Loads application

External tectonic forces were treated as model variables, thus their gradual refining allowed for an evaluation of the role of each singular factor in the complex system. They were imposed on the boundary segments as: (1) constant pressure, (2) linearly varying pressure and occasionally (3) forces exerted directly to selected nodes. The last option was useful for areas where S_{Hmax} trends obliquely to the model boundary. The fast and easy way of the boundary pressure modification permits hundreds of force configurations to be tested.

We also incorporated a correction for topographic stresses assumed to arise from density structure variations within the isostatically balanced lithosphere. The influence of lateral density variation is proportional to the density moment of the mass dipole formed by the mass anomaly (Fleitout 1991; Ranalli 1995). The horizontal volume force, proportional to the horizontal gradient of the density moment (Fleitout 1991) was calculated by Coblentz *et al.* (1994) as the gravitational potential energy difference across each element and subsequently applied as a force to nodes. In our model this concept is also adopted, although implemented in a different way. At first, the correction was calculated for each element as a difference between gravitational potential energy of given element and the reference state (eqs 1 and 2). Then, this correction was applied as pressure on each element's fringe (Fig. 5). The positive gravitational energy generated by elevated areas was reproduced by a pressure directed outwards of the element, whereas negative energy, generated by marine depressions was directed inwards of the element. A disadvantage of this method in comparison to the one mentioned above (Coblentz *et al.* 1994), is that pressures are applied perpendicularly to the element's fringes instead parallel to the maximum energy gradient. However, fine mesh used in our model minimizes this negative effect. The correctness of this approach was verified by comparison with the benchmark presented by Bada *et al.* (2001).

The reference lithosphere, for which no correction is assumed, has an altitude (h) within the range of ±300 m over/below sea level and a $z_0 = 30$ km thick continental crust. This simplified assumption is valid for the Palaeozoic platform of Central Europe, where results of deep seismic refraction profiles typically show 28–32 km crustal thickness (Ansogre *et al.* 1992; Thybo 2000; Guterch *et al.* 1994, 2003). However, this assumption is not valid for the EEC where the crust is *ca.* 40 km thick, and for the centre of Pannonian basin, having 26-km-thick crust (Horváth 1993). In the latter cases, the deviation of crustal thickness from the reference is partially compensated by variations of intracrustal density. The thick crust of the EEC is somewhat compensated by a heavy mafic lower crust (Królikowski & Petecki 1997), and the thin Pannonian crust, by a thick and light sedimentary layer (Lillie *et al.* 1994). Our estimates indicate that differences in the potential energy due to lateral density variations in the crust without relief are negligible in comparison to the effect of, for example, 0.5 km isostatically balanced elevation.

The adopted density characteristics of the lithosphere are: crustal density $\rho_c = 2750$ kg m^{-3}, and upper mantle density $\rho_m = 3300$ kg m^{-3} (Andeweg, 2002). For two types of lithospheric structure a correction was carried out:

(1) continental crust with topography over 300 m and
(2) continental crust bearing intracontinental basins filled with water of density $\rho_w = 1000$ kg m^{-3}.

The correction for elevated areas (F_L) and intracontinental basins (F_M) is expressed by formulae:

$$F_L = 0.5g\rho_c h^2 + g\rho_c h z_0 + g\rho_c^2 h^2 / 2(\rho_m - \rho_c), \quad (1)$$

$$F_M = 0.5g(\rho_c - \rho_w)h^2 - g(\rho_c - \rho_w)hz_0 + g(\rho_c - \rho_w)^2 h^2/2(\rho_m - \rho_c). \quad (2)$$

As an example of a topographic correction: 1 km of elevated orogen with its crustal roots produces an outward push of 0.9×10^{12} N m^{-1} for each element. Alternatively, 1 km of deep intracontinental basin filled with water generates an inward directed pull of 0.53×10^{12} N m^{-1}. To calculate the topographic pressure on the element fringe, these forces were averaged over the thickness of a given tectonic unit.

4 PRINCIPAL MODEL CONSTRAINTS: STRESS DIRECTIONS AND STRESS REGIMES

All numerical models investigated in this study are constrained by the S_{Hmax} directions to a depth of 70 km taken from the World Stress

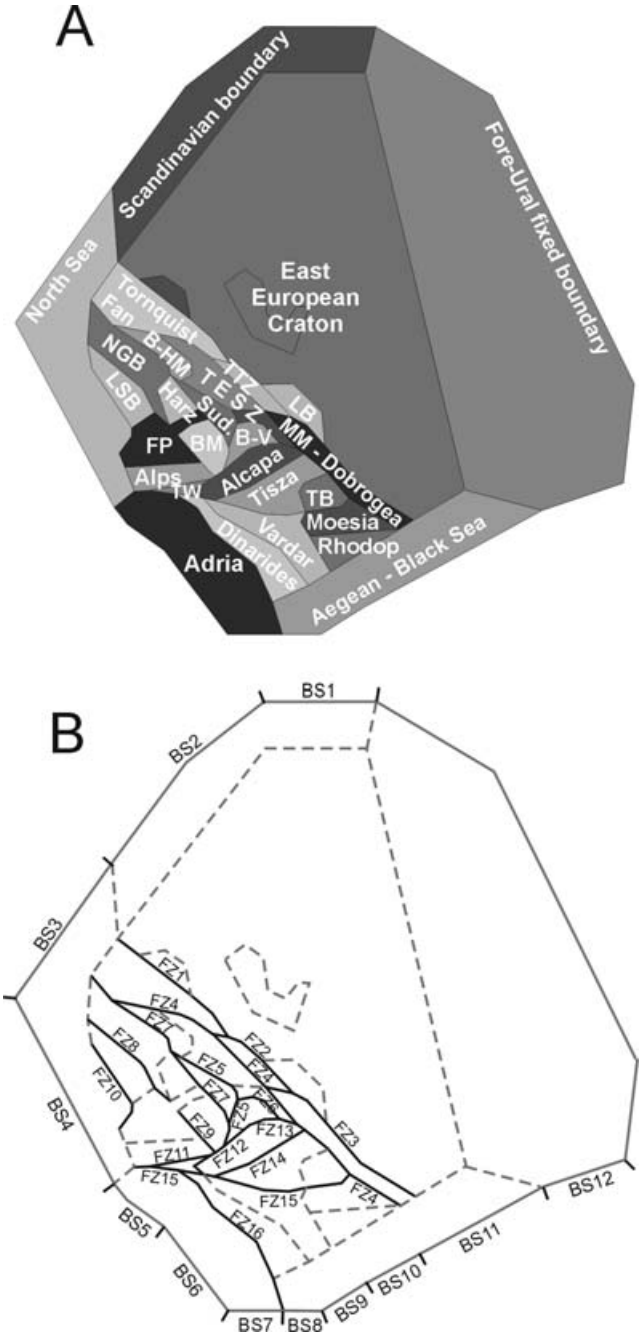

Figure 4. Structural elements of the models: (a) Tectono-mechanical units: BM—Bohemian massif; B-V— Bruno-Vistulicum massif; FP—Franconian platform; LB—Lublin basin; LSB—Lower Saxony basin; MM—Małopolska massif; NGB—North German basin; TB—Transylvanian basin; TTZ—Teisseyre-Tornquist zone; TW—Tauern Window (Table 2). (b) Fault zones and boundary segments; solid lines—faults; dashed lines—continuous boundary between tectonic units; for abbreviations see Tables 3 and 5).

Map database (Reinecker *et al.* 2003), supplemented with data from Roth & Fleckenstein (2001) and Jarosiński (2005a) (Fig. 4). To enable a visual judgement of modelling results versus observations, smoothed S_{Hmax} trajectories are drawn in places where the data show clear trends of stress direction. Dashed trajectories indicate places where S_{Hmax} directions are poorly constrained or scattered.

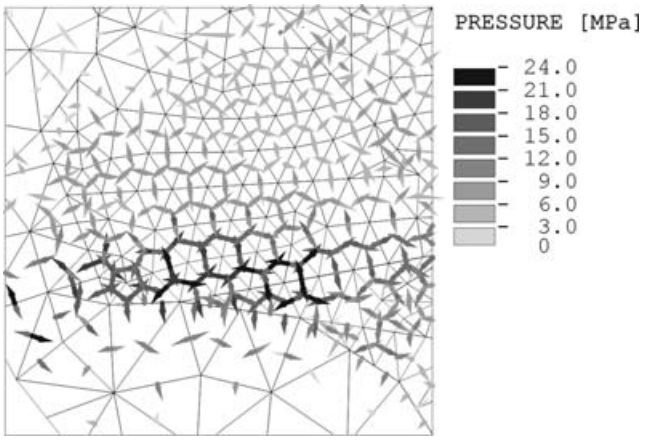

Figure 5. Correction for topography-related stresses for the Alps and the adjacent areas. For location see the white square in Fig. 3. The correction has the magnitude equals to the gravitational potential energy difference between the element and the reference model of the lithosphere. It is applied as a pressure exerted to the side of each element. The length of bars and the grey scale indicate the pressures averaged over the lithospheric thickness.

In ambiguous cases, published results of a smoothing procedure by Gerner *et al.* (1999) and Müller *et al.* (1997) were taken into account.

The areas with best-constrained stress trajectories are selected to test model predictions against observations. In general, the stress trajectories across Europe form two large-scale arches converging in the Dinarides (Fig. 2). The northern arch passes through the Alcapa, the Małopolska massif and the EEC margin in western Scandinavia. The southern arch crosses the Pannonian basin, the Moesian and Scytian platforms and the Black Sea up to the Pontides. The Aegean extensional province is located in the centre of the southern arch. The principal condition for a numerical model to be considered successful was a good reproduction of this characteristic arch shape geometry of the intraplate stress trajectories across Europe. Secondly, a good prediction of the locations of the stress triple junctions in Ukraine was required.

Stress regimes were also utilized as model constraint. Since there is no simple relation between the stress regime in the lithosphere and the stress vectors in a plane stress model some assumptions have to be made. We assume that without tectonic and topographic loads the lithostatic state of stress stabilizes and due to inelastic stress relaxation will be close to hydrostatic. Regarding the long-term strength of the rock, the horizontal stress component (S_{HV}), produced by side expansion of the rock, is lower than the overburden pressure (S_V). This implies that a static lithosphere is in a weak extensional state of stress. Assuming that there is a parameter A: $S_{HV} + A = S_V$, a compressive stress regime may develop only when the tectonic stress component $S_H > A$. The value of A is dependent on the rheological state of the lithosphere, and thus will change from site to site. Since A is unknown for a given element of the model it is not possible to ascribe unequivocally the stress regime from the computed tectonic stresses. Therefore, only some general rules can be formulated:

(1) when both tectonic stress components are extensional ($S_H < 0$ and $S_H < 0$) or in the case of the absolute value of extension higher than compression ($/S_h/ > /S_H/$) the stress regime is always normal fault,

(2) an extensional stress regime is likely when the tectonic stress contribution is small, even if compressive,

(3) only when both tectonic stress components are highly compressive, a thrust fault stress regime is possible and

(4) when S_H is highly compressive and $/S_h/ < /S_H/$, a strike-slip fault regime is the most probable. Although in a plane stress model one cannot discriminate between stress regimes, it is nevertheless possible to make a good guess, which stress regime is most likely, using the above concept.

5 MODELLING PROCEDURE AND GROWING COMPLEXITY OF THE MODELS

Forward modelling with a trial-and-error procedure was used to obtain the best fit of the computed S_H directions to the measured S_{Hmax}. The best fit was judged, first of all by a comparison with the reference sites where the stress field is best constrained. The only constant attribute of the model is geometry—boundary, areas, fault zones and mesh. Another features, like loads on the boundary, topographic stresses, material properties and friction coefficient on the faults are variables. To examine the influence of separate factors on S_{Hmax} distribution, four sets of models with increasing complexity were designed. Within each set we tested several models with different boundary conditions (see Table 4). The boundary loads obtained by the best fit of the more simple models served as the starting point for the more complex ones. A preliminary model M0 was designed to test a simple shape of the model. We found that the location of the 'stress triple junction' cannot be reproduced properly using the simplified geometry of the Adria-Dinaric suture, approximated by a straight line. An updated geometry was adopted for the models Mod1–Mod8 (Table 4), which are described hereafter.

The **first set of models (M1)** was designed with a constant elastic thickness of the lithosphere (100 km), constant material properties ($E = 70$ GPa), absence of topographic stresses and locked faults by applying coefficient of friction $\mu = 1$. To establish initial conditions for the model, ridge push on the NW passive margin was applied conforming with Gölke & Coblentz (1996), Andeweg (2002) and Goes *et al.* (2000) in the range of 10–20 MPa. The first finding of this simple model was that the complex stress pattern in Central Europe could not be reproduced easily, suggesting that the configuration of the boundary forces is quite unique. Using the simple Mod1 only an overall double-arch trend of S_H was possible to predict (Fig. 6). The basic requirement to predict a proper location of the 'stress triple junction' was high tension at the Greece and the Aegean boundary segments (BS8 and BS9).

The **second type of model (M2),** includes either the correction for topography-induced stresses or unlocked faults but no topography-induced stresses. Computing these models with the boundary loads from the Mod1 led to essentially incompatible results. More compression had to be put to the NW and SE boundary to sustain topography-related compression or to compensate for faults motion (compare Mod1 and Mod2, Mod3, Table 5). Implementation of topographic stresses allows to calibrate the magnitude of the boundary forces by equilibration of stress regimes in the high mountain ranges. In the Scandinavian Mts. and the Alps, the S_H direction changes from perpendicular to parallel with respect to the orogen chain (Fig. 6). However, topographic stress component has negligible effect on S_H orientation out of the elevated areas. In the containing faults Mod3, at the beginning we tried constant average friction coefficient for all faults. In this case it was not possible to resolve the model because we obtained movement on actually inactive faults and vice versa. To avoid the mismatch we had to adjust friction coefficient of each fault separately. It appears that local stress rotations as well as rapid stress regime and magnitude changes are correlated with active faults (Fig. 6). This appears to be the main factor governing the second-order stress pattern.

Table 4. Configuration of models.

Set of model	Model	Including topography	Including faults	Stiffness contrast	W Europe side loading
M1	Mod1	No	No	No	Compressive
M2	Mod2	Yes	No	No	Compressive
	Mod3	No	Yes	No	Compressive
M3	Mod4	Yes	Yes	No	Compressive
	Mod5	Yes	Yes	No	Strong tension
M4	Mod6	Yes	Yes	Low	Free boundary
	Mod7	Yes	Yes	Moderate	Slight tension
	Mod8	Yes	Yes	High	Slight tension

The **third set of models (M3)** includes both faults and topography-related stresses. Comparison of fault models without and with topographic stresses shows that the second one is tighter. For fixed friction coefficients, the addition of the bulk of topography-related forces reduces fault displacement by *ca.* 50 per cent. This effect can also be illustrated by a comparison of coefficients of friction that are necessary to maintain equal fault displacements in Mod3 and Mod4 (Table 3). We tested a spectrum of models varying from a tight compressive one (Mod4) to a relaxed one (Mod5). For the compressive model, a more uniform stress field was acquired but active faults need extremely low friction coefficients (Table 3). A slightly compressive stress regime in the Alps indicates that the boundary forces are overestimated. In the relaxed model, it can be shown that the stress field breaks apart into domains characterized by divergent stress magnitudes, directions and regimes (Fig. 6) when the loads are underestimated. One of the main findings of these models was that the friction coefficient at faults should be precisely adjusted to obtain a good solution. For example, the effectiveness of stress transmission from the Adria indenter to the interior of Europe is strongly dependent on the friction coefficient of the Dinaric suture. When a too high friction is assumed ($\mu > 0.6$), the indenter becomes less mobile, which limits the amount of strain energy transmitted to the Alpine foreland and results in energy deficit in the Pannonian–Dinaric region. In the case of too low friction ($\mu < 0.4$), more strain energy transmitted to the Alps is paid with energy deficit in the Pannonian–Dinaric area.

In the **fourth set of models (M4)** material properties were modified between tectonic units to investigate the range of mechanical contrasts for which a satisfactory model's solution was possible. The maximum difference of stiffness (*Sf*—see Section 3.1) was always identified between the weakest Pannonian basin (Tisza) and the most rigid EEC. In the first step, when a moderate mechanical contrast was implemented (Table 2: Mod6 and Mod7), the model became less tight relative to the analogue with uniform mechanical properties. Further increase of stiffness contrast between tectonic units results in an increase of required fault friction (compare Mod7 and Mod8, Table 3). The Mod 8 has the maximum acceptable stiffness contrast in a range of 1×10^{15} Pa*m to 9×10^{15} Pa*m. Too high stiffness contrast between rigid massifs (Bohemia, Upper Silesia, Moesia) surrounding the weak Pannonian basin is the reason for S_H rotation to position tangentially with respect to the borders of this mechanically soft inclusion. This is not the case for the S_{Hmax} in this area. In addition, too weak Alcapa block is unable to transmit NE-oriented S_H further into the EEC in order to reproduce the stress

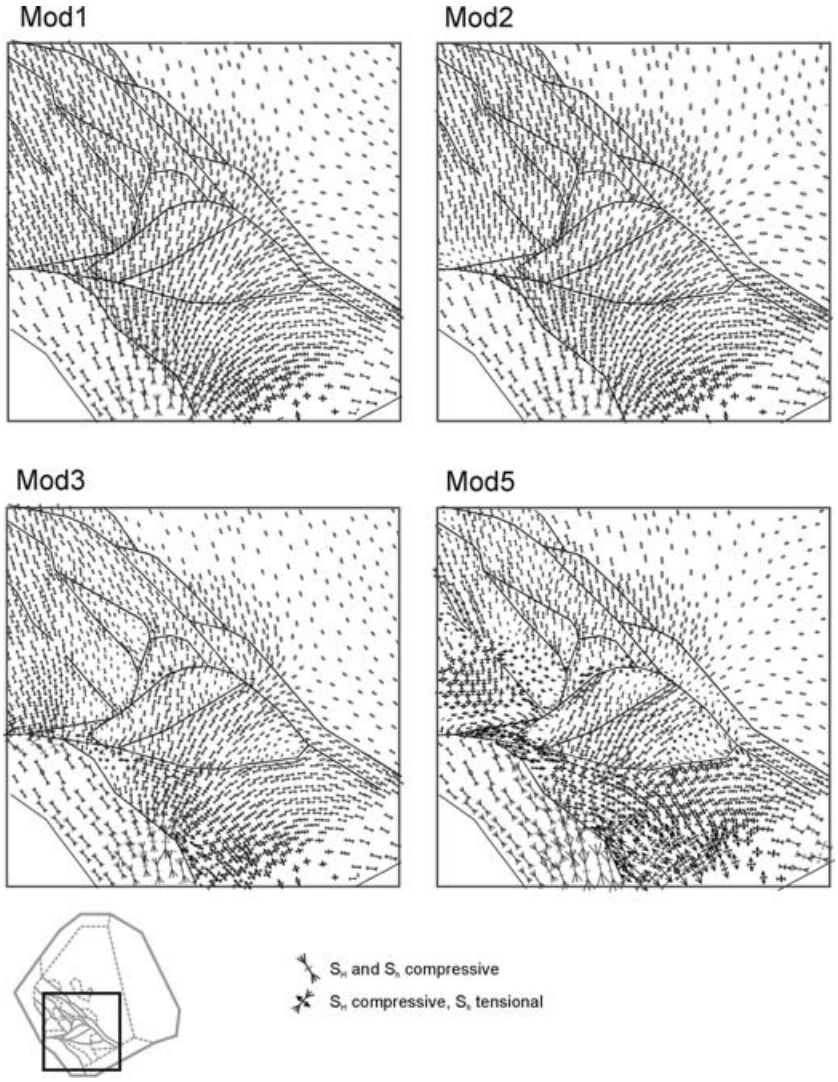

Figure 6. Results of S_H distribution for the best-fitted solutions of models with constant stiffness. Mod1—mechanically uniform model, Mod2—model containing topography-related stresses, Mod3—model with faults, Mod5—model containing topography-related stresses and faults. For more details of models configuration see Table 4.

Table 5. Boundary segments and external tectonic pressures.

Boundary Segment		Mod1	Mod2	Mod3	Mod4	Mod5	Mod6	**Mod7**
BS1	Barents Sea	13	15	14	16	8	13	**10**
BS2	Norwegian Sea	11	13	12	13	6	11	**8**
BS3	North Sea	16 → 14	19 → 16	17 → 15	19 → 16	13 → 8	16 → 14	**14 → 12**
BS4	British–French	6	4	4	4	−4	0	**−2**
BS5	Alpine	8	8	8	8	2	6	**4**
BS6	Apennine	6	4.5	6.5	6.5	−1.5	4	**0**
BS7	Ionian Sea	75	80	82	80	71	82	**74**
BS8	Greece	−12 → −23	−10 → −20	−12 → −23	−10 → −20	−14 → −26	−10 → −20	**−12 → −22**
BS9	Aegean Sea	−23	−18	−24	−20	−26	−20	**−22**
BS10	Marmara Sea	−8 → 16	−6 → 14	−19 → 20	−8 → 14	−16 → 14	−17 → 21	**−20 → 22**
BS11	Black Sea	18 → 7	30 → 14	22 → 7	32 → 16	22 → 7	24 → 10	**24 → 10**
BS12	Caucasus	10 → 15	10 → 15	10 → 15	10 → 15	4 → 8	8–12	**6 → 10**

Tectonic pressures are normalized per 100-km-thick lithosphere and given in MPa.
→ points to linear variation of external tectonic pressure from W to E within given boundary segment.

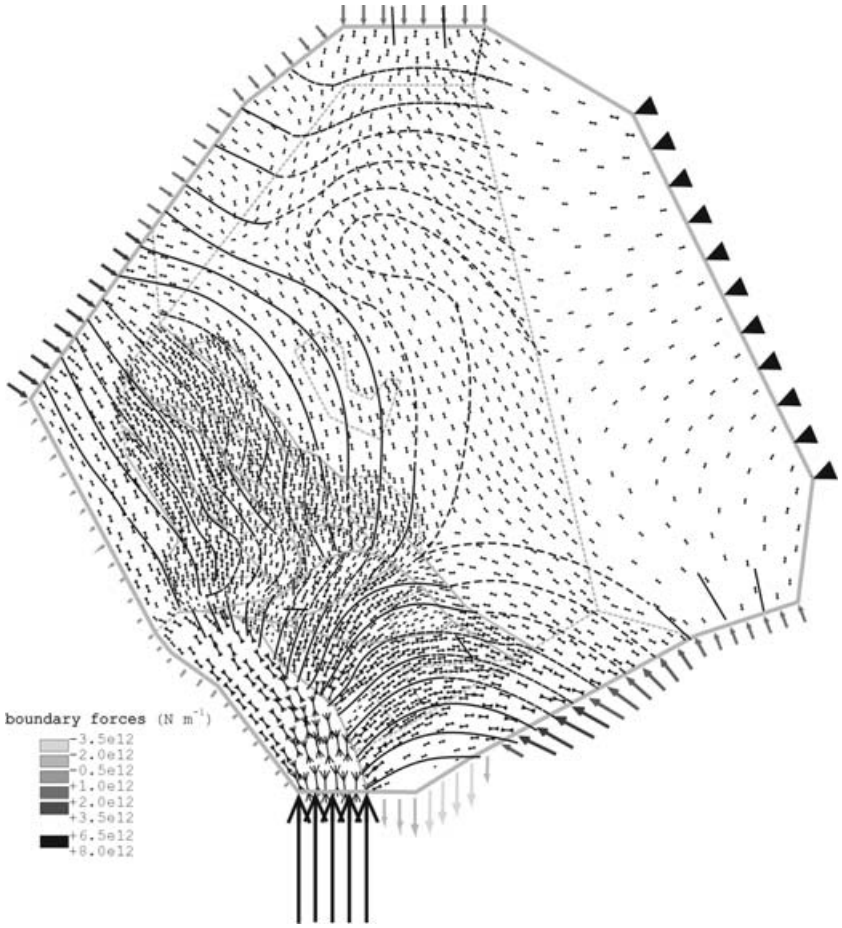

Figure 7. Predicted S_H directions and boundary loads for the Mod4 with uniform stiffness, which comprises faults and topography-related stresses (compressive case). Size of external arrows is proportional to the boundary forces, which are also expressed by the grey scale. Where the arrows are perpendicular to the boundary, the loads are applied as a pressure, where they are oblique the loads are implemented as a combination of pressure exerted to the lines and forces applied to the nodes.

pattern within the craton. Obtained maximum stiffness contrast of one order of magnitude is similar to the integrated strength contrast predicted for this region from a rheological study (Lankreijer *et al.* 1999).

6 THE ORIGIN AND STATE OF TECTONIC STRESS IN CENTRAL EUROPE: DISCUSSION

6.1 The concordance between models and data

Although all models fit well the general double-arch pattern of S_{Hmax}, the most accurate solution has been obtained for Mod4 with uniform stiffness (Fig. 7), and Mod7 with variable stiffness (Figs 8, 9 and 10). Below, we describe the results of our preferred and most complex Mod7. Predicted S_H directions fit the data satisfactorily for western Scandinavia, where the characteristic distortion of S_{Hmax} from W–E in the North Sea to NNW–SSE for the Baltic Sea is correctly predicted (Fig. 7). By testing several loading scenarios we found that this stress distortion is mostly controlled by a drop of the ridge push magnitude from the North Sea to the Norwegian Sea segment. In central Fennoscandia most data show a circumferential S_{Hmax} pattern around the Gulf of Bothnia, which is the centre of post-glacial uplift. In this area misfit between the model and the data was unavoidable because of lack of flexural stresses in our 2-D model. For the Scandinavian Mts., the S_H rotation towards the NE–SW is comparable to the S_{Hmax} data, although of low quality (Henderson 1991). For Fennoscandia a compressive stress was inferred in both horizontal directions, therefore either strike-slip or thrust fault stress regimes are plausible, which accords with the data (Stephansson *et al.* 1991).

In the Palaeozoic platform of Western Europe, a dominant NW–SE S_{Hmax} direction and a fan-like pattern of stress in the foreland of the Alps (Reinecker *et al.* 2003) is predicted satisfactorily (Fig. 8). However, in the westernmost Bohemian massif and the Eger graben our results point to N-oriented S_H while borehole data show a consistent NW–SE S_{Hmax} direction. Because a good fit between model and the data could not be reproduced by any of our FEM models some additional factors not included in the model have to be considered, for example, the mantle plume below the Eger Graben (Špičák *et al.* 1999). For northeastern Germany and northwestern Poland, where stress partitioning between tectonic levels is postulated (Roth & Fleckenstein 2001; Jarosiński 1999), we obtain S_H direction, which is the mean for these levels. According to the data, the stress regime in Western Europe is mosaic-like with a dominance of compressive regimes (Müller *et al.* 1997). In our model the horizontal stress is close to uniaxial. Taking into account that the absolute values of compressive S_H always exceed extensional

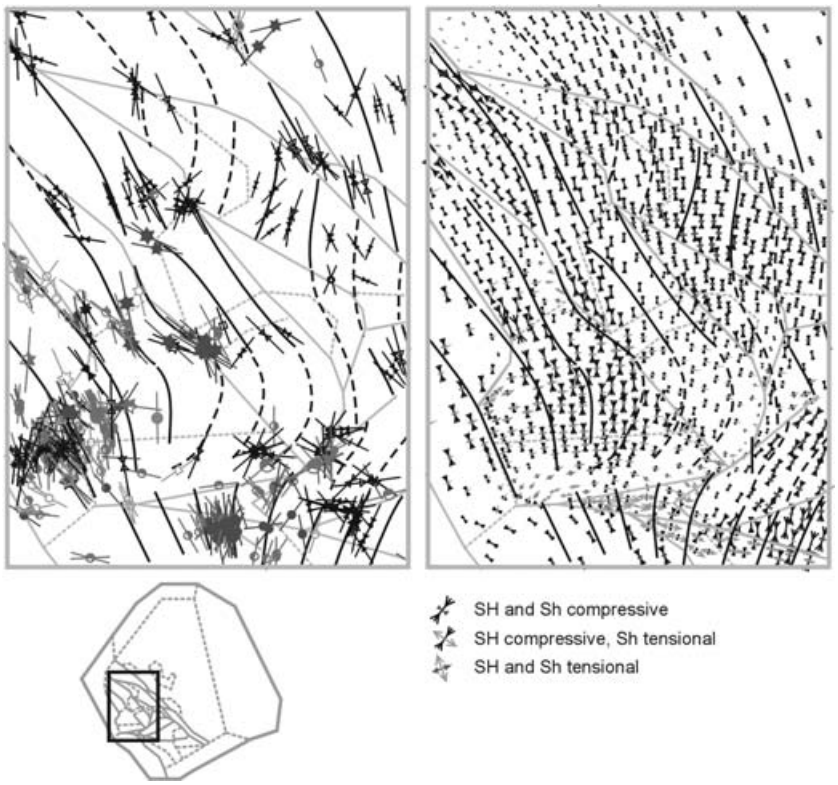

Figure 8. Comparison of the data and modelling results (Mod7) from the Alps and the Palaeozoic platform of Central Europe. For explanation of symbols used for S_{Hmax} data see Fig. 2.

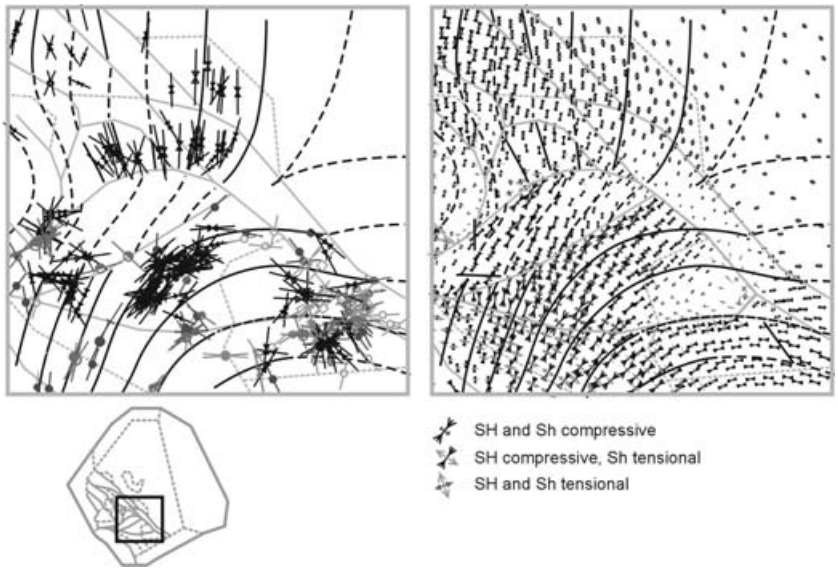

Figure 9. Comparison of the data and modelling results (Mod7) from the Carpathians, their foreland and the Pannonian region. For explanation of symbols used for S_{Hmax} data see Fig. 2.

S_H, the strike-slip stress regime is the most probable. Normal fault stress regime is predicted for the Alps with the most pronounced longitudinal extension of the Tauern Window. The obtained results are consistent with the present-day tectonic setting compiled for the Central and Eastern Alps by Selverstone (2005). Comparison of tectonic and topography-related stresses from different models led us to conclusion that extension and escape of the Tauern Window is principally due to the Adria push as the principal reason.

In eastern Poland, the observed small S_{Hmax} deviation from NNE–SSW in the Carpathian foreland to NNW–SSE in the Baltic Sea is correctly reproduced (Fig. 7). This southwestern margin of the EEC appears to be a sensitive spot of the model. Relatively small changes in boundary loads turn S_H either parallel or perpendicular to the edge of craton. The fan-like pattern of S_{Hmax} in the autochthonous basement of the Outer Carpathians is also correctly predicted in the model (Figs 7 and 9). In the Bruno-Vistulicum segment of the

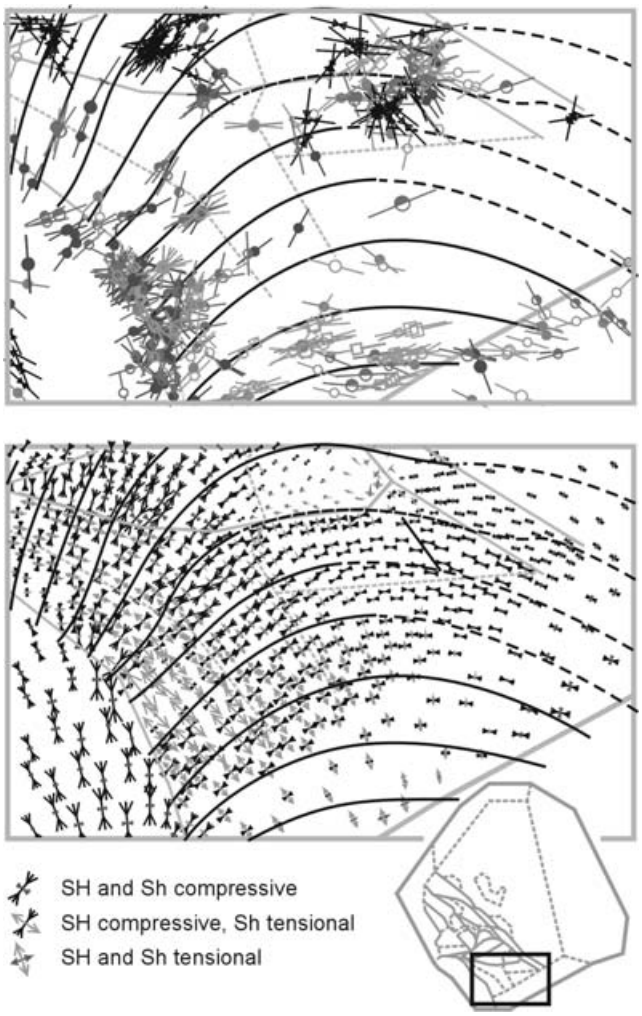

Figure 10. Comparison of the data and modelling results (Mod7) from the Greece–Aegean region. For explanation of symbols used for S_{Hmax} data see Fig. 2.

Carpathians, the modelled N–S direction of S_H is an intermediate between the observed S_{Hmax} directions for the Carpathian nappes and their basement (Jarosiński 1998). Here, the effect of accommodation of the sinistral Mur-Žilina fault segment (FZ12) is observable. This effect is possible only when low friction coefficient is assumed for this fault zone. In entire Poland both tectonic stress components are compressive, with significant dominance of S_H. This implies that a strike-slip stress regime is most likely, which is in agreement with stress measurements from mini-fracturing tests in deep boreholes in Poland (Jarosiński 2005b).

In the Carpathian–Pannonian area, the calculated S_H directions match the S_{Hmax} data satisfactorily. In the southern part of this region the stress arch between the Dinarides and the Black Sea is well expressed. Due to the large magnitude of both horizontal stresses in the southern part of the Tisza block a thrust fault stress regime is likely here, conforming the observations (Gerner *et al.* 1999). In the rest of the Tisza block, as well as in the Alcapa block a strike-slip stress regime is more probable due to a small value of the S_H. Only in the Eastern Carpathians and southern Transylvania low tectonic stresses in both directions make an extensional stress regime possible. In northern Transylvania, high magnitudes of uniaxial tectonic stress promote strike-slip stress regime. The Southern Carpathians are exposed to high tectonic stress, exceeding the topography-related extension, and resulting in highly compressive S_H and slightly extensional S_H. This suggests a strike-slip stress regime, which also emerges from the focal mechanism data (Radulian *et al.* 2000). The eastern segment of the mid-Hungarian fault, reveals some degree of stress partitioning marked by the S_H shift from NE–SW to NNE–SSW (FZ14). Windhoffer *et al.* (2003) gave some explanation of this phenomenon.

For the Balkan area, a satisfactory match between modelled S_H directions and S_{Hmax} data was obtained. Superposition of the Adria push and the Aegean extension enhanced by topographic extension of the Dinarides causes dramatic changes in the stress regime and its magnitude (Fig. 10). The largest compressive S_H are predicted for the foreland of the Dinarides. In the northern segment of the foreland, where a NE-oriented S_H is transmitted towards the Pannonian region, the compressive S_H is much higher than the absolute value of extensional S_H, thus a strike-slip stress regime is the most probable in this region. The same stress regime but less compressive can be ascribed to the Moesian platform and the Rhodope Mts. An extensional stress regime, characterized by small S_H and highly extensional S_H, was obtained for the southern Dinarides, their foreland and the Aegean region. The transition from the Aegean towards the Black Sea is connected with gradual change of the stress regime into a compressive one. According to the modelling results, the specific combination of thrust fault and normal fault stress regime, which is also demonstrated by focal mechanism data for the Southern Dinarides (Anderson & Jackson 1987; Reinecker *et al.* 2003), can be interpreted as the stress partitioning across the suture between Adria (compressive) and the Dinaric-Aegean (extensional) stress domains. Systematic stress regime partitioning is also predicted across the Periadriatic–Drava line, where the strike-slip stress regime in the Dinaric foreland switches to thrust fault in the southern part of Tisza.

6.2 Balance between boundary forces

In this study we have tried hundreds of configurations of boundary forces, some of which can even be considered extreme, to check the uniqueness of the models' solution. By including gravitational potential energy and by considering only realistic stress regimes, we limit the number of acceptable model solutions. It was verified that, even if the absolute values of stresses are not correctly weighted by a rough estimation of topographic stress, the differences between loads at the boundary segments are kept constant for a wide range of models. The adopted values of the final boundary loads are presented in Table 5. The scope of the preferential solution for boundary loads is between the Mod6 and Mod7. The difference between ultimate values of acceptable boundary loads is typically less than 0, 2×10^{12} N m^{-1} (= 2 MPa of tectonic pressure over 100-km-thick lithosphere) and does not exceed 0, 4×10^{12} N m^{-1} (4 MPa per 100 km). To simplify the presentation of the modelling, only results of the Mod7 are described extensively hereafter.

The obtained tectonic pressure on the NE passive margin of Europe ranges 8–14 MPa. According to analytic calculations by Andeweg (2002) the 30–80-Ma-old oceanic lithosphere should produce a ridge push in the range of 10–25 MPa. When an effect of *ca.* 10 MPa of continental margin extension is subtracted from this value, the pressure at sea level drops below 15 MPa. This is in the same range as calculated by means of distributed ridge push integrated over the Atlantic Ocean plate (Gölke & Coblentz 1996; Andeveg 2002). Overcoring measurements in mid-Norway and near the Oslo graben show similar tectonic (differential) stresses in the

range of 10–20 MPa (Fejerskov & Lindholm 2000). Theoretically, the ridge push should decrease in the direction of decreasing age of the ocean floor. Our solution follows this trend with considerable drop of pressure from the North Sea segment (**BS3 –**14–12 MPa) to the Norwegian Sea segment (**BS2 –** 8 MPa), which appears to be necessary to obtain characteristic bend of S_{Hmax} in western Scandinavia. A rapid jump of loads between these segments is possible due to the presence of a major fracture zone, separating the Mohna ridge from the Iceland ridge. The trend of north-eastward decrease of ridge push is not held when proceeding further into the Barents Sea. The best solutions of the models give systematically higher compression at the Barents Sea (**BS1 –**10 MPa) than at the Norwegian Sea segment (Table 5). The same comes out from overcoring, which indicated 15–25 MPa of tectonic stress for northern Norway (Finnmark) and 10–15 MPa for western Norway (Dart *et al.* 1995; Fejerskov & Lindholm 2000). The higher level of compression in the Barents Sea points to more intensive push of the Arctic Ocean than for the Norwegian segment of the Atlantic.

A precise balancing of loads in the British–French segment (**BS4**) is important for S_H adjustment at the edge of the EEC. For instance, an increase of tectonic pressure by only 2 MPa rotates the stresses perpendicular to the edge of the EEC. A decrease by the same amount turns S_H parallel to the craton margin. The preferential solution gave slight tension or free boundary conditions (0–2 MPa) in the direction perpendicular to S_H. Such solution seems reliable at least at the French segment, because both strike-slip and normal fault stress regimes dominate the Rhine graben area (Plenefisch & Bonjer 1997).

For the Apenninic segment (**BS6**), a free boundary or a weak compression is predicted (0–4 MPa). We found that applying higher compression on this segment leads to destruction of sensitive stress pattern in the Aegean–Pannonian region and results in extremely low friction coefficients at active faults ($\mu < 0.1$). The free boundary solution suggests that slab pull of the retreating western Adria (Rosenbaum & Lister 2004) and tectonic push are in equilibrium in the Apennines, when calibrated to the sea level.

Our modelling study shows that a strong push at the Ionian Sea segment (**BS7**) of the Adriatic block is crucial for the stress distribution in Central Europe. First of all, it is responsible for the northward advance of Adria relative to the rest of Europe. Due to eccentricity between collision resistive forces in the Alps on one side, and the Ionian Sea push on the other side, Adria rotates counter-clockwise. The complex stress arrangement in the Carpathian–Pannonian region and the edge of the EEC is sensitive even to ±2 MPa changes in this compression. The acquired tectonic pressure of 74 MPa is several times larger than the pressure at any other segment of the model. Taking into account that this push is exerted to a 4-km-deep marine basin, this load may increase to more than 90 MPa when adjusted to the reference sea level. Excessive collision-related stresses indicate that Adria is mechanically coupled with the African plate and, in this sense, can be regarded as the African promontory. This stress concentration is possible due to the lack of strain accommodation within the narrow corridor between the Calabrian and the Hellenic subduction zones.

Considering the force torque, a high level of extension at the Greece–Aegean segment (**BS8+BS9**), in the range of 20–22 MPa, balances the Ionian Sea compression. The northern range of the Aegean extensional province and the shape of the southern stress bow are strongly dependent on the loads applied to this extensional segment. A significant amount of extension suggests contribution of the slab pull from the Hellenic subduction zone in addition to the topographic pull of the Aegean Sea margin. This conclusion parallels results of modelling by Flerit *et al.* (2004), who claimed that the Hellenic arc-pull produces N–S extension in the Aegean and drives southwestward escape of the Anatolian block.

As suggested by GPS and focal mechanism data (Reilinger *et al.* 1997; Kotzev *et al.* 2001), the short Marmara Sea segment (**BS10**) is a transition area between the Aegean extensional domain and the Black Sea compressional domain. Transition from 20 MPa of extension to 22 MPa of compression, respectively, is predicted in our model. At the Black Sea segment (**BS11**) tectonic loads are applied obliquely to the model border. It should be mentioned that this is not a predefined assumption but a necessary condition to obtain the best-fitted model. A westward-oriented component of push may result from friction along the dextral North Anatolian fault. Another prominent feature of the Black Sea segment is a significant decrease of tectonic push eastwards, from 24 MPa to 10 MPa. It can be estimated that approximately half of this difference is an artificial effect of crossing a deep sedimentary basin by the model's boundary. Using thermo-mechanical modelling, Cloetingh *et al.* (2003) show that the eastern part of the Black Sea is mechanically weaker than the western part and, therefore, less efficient in stress transmission towards the EEC. This may explain the observed eastward decrease in tectonic push in the Black Sea area. Also earthquakes are stronger in the western Pontian segment of the North Anatolian fault than in the more eastern one (Kahle *et al.* 2000).

The Caucasus segment (BS12) is located in the peripheral part of the model, close to the fixed boundary, and for this reason loads are constrained with lower precision then elsewhere. However, the established small tectonic pressure of 6–10 MPa, could not vary in a wide range of magnitudes because stress directions in front of the Urals and at the edge of the EEC are still sensitive to these changes. Minor tectonic push from the Caucasus orogen can be seen in deformation models constrained by the GPS measurements and seismology (Reilinger *et al.* 1997; McClusky *et al.* 2000), which show that the relatively fast northward advance of Arabia is compensated by the westward escape of the Anatolian block and by ongoing contraction in the Great Caucasus. In consequence only a minor portion of the Arabian push is transmitted into the EEC interior.

6.3 Stress magnitude

To demonstrate the effect of mechanical differentiation between tectonic blocks on the stress variation within the lithosphere, two end-member models are presented: one mechanically uniform model with a 100-km-thick lithosphere (**Mod4**) and the other with moderate stiffness/thickness variations between tectonic units (**Mod7**). A positive topography (elevated areas) produces extension within the elevated mountain chains and compression at surrounding lowlands. Intracontinental marine basins have the opposite effect: produce compression in their interiors and extension in their flanks. For example, in the Alps topographic extension reaches the maximum of $2.5{*}10^{12}$ N m^{-1}, with an average in the range of $1.0–1.5{*}10^{12}$ N m^{-1} (Fig. 11). For most of the Dinarides and the Carpathians this extension is in the range of $0.5–1.0{*}10^{12}$ N m^{-1}. Compression within the deepest sedimentary basins attains $0.5{*}10^{12}$ N m^{-1} in the Adriatic Sea, and $1.2{*}10^{12}$ N m^{-1} in the Black Sea. These numbers demonstrate that the highest topographic anomalies provide stresses in the same order as the North Atlantic ridge push at the reference sea level. However, topographic stresses mainly affect the elevated or depressed areas but they have only limited influence on neighbouring areas. According to predictions by Bada *et al.* (2001),

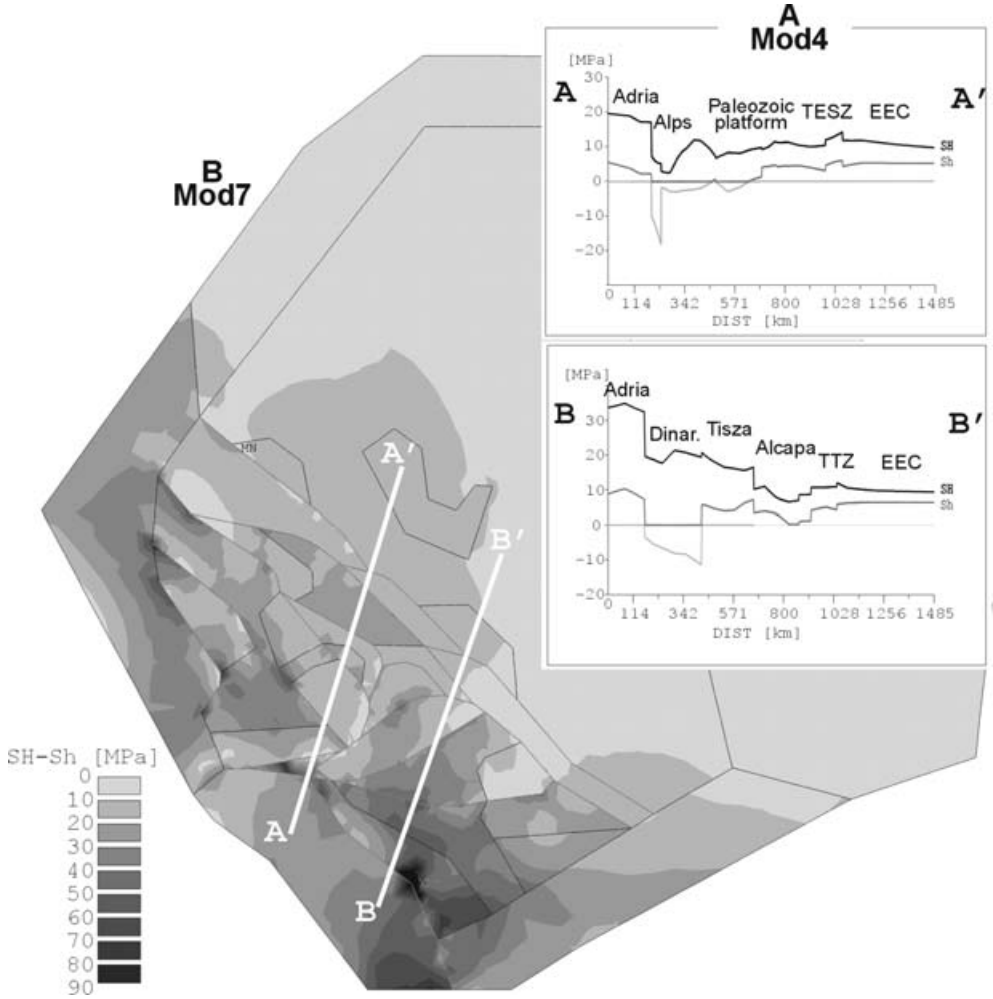

Figure 11. Stress magnitudes: (a) curves of S_H and S_H for Mod4 with constant thickness—stresses are averaged over 100-km-thick lithosphere (location at Fig. 11b); (b) map of differential horizontal stress magnitude for Mod7 with variable stiffness of tectonic units—stresses are averaged relatively to the thickness of a given tectonic unit (see Table 2).

less than $0.2^{*}10^{12}$ N m^{-1} of compression is exerted to the Pannonian basin due to the push from surrounding mountain chains.

Stress magnitudes in the 100-km-thick model are displayed in two sections (Fig. 11). In the transect passing through Adria, the Alps, Palaeozoic platform of Central Europe and the EEC, the most compressive S_H, up to 20 MPa, is attained in the northern part of the Adria indenter. In the Alps, due to stress partitioning at the Periadriatic line and to topographic extension, compression drops to less than 5 MPa. In the Alpine foreland the S_H magnitude rises again over 10 MPa and keeps a relatively stable magnitude in the range of 10 ± 3 MPa in the rest of the plate. Extensional S_H develops only in the Alps and their foreland. At the eastern line passing through Adria, the Dinarides, the Pannonian basin, the Carpathians and the EEC, the highest S_H, over 30 MPa, is computed for the centre of the Adria indenter. Stress partitioning at the suture and topographic stresses cause the compression drop below 20 MPa in the Dinarides, which however raises slightly over 20 MPa in front of this orogen. In the Pannonian region S_H decreases to 15 MPa within the Tisza block and falls down rapidly below 10 MPa in the Alcapa block and the Carpathians. The stress drop is caused by displacement along the mid-Hungarian fault zone. The Carpathian foreland and the EEC undergo compression close to 10 MPa. Extensional S_H, in the range of 5–10 MPa, is predicted for the Dinarides and their foreland. The domain with an tensional stress component reaches the Periadriatic–Drava Line, where it switches rapidly into compression in the Tisza block. The Aegean extensional agent is unable to cross this major tectonic fault zone.

For the second model, with a mechanically heterogeneous lithosphere, differential stresses are presented in a map (Fig. 11). The general rule is that stresses are more concentrated when the plate becomes thinner, but at the same time, they are slightly reduced in magnitude due to the systematic decrease of Young's modulus in the thinner lithosphere (Table 2). The highest differential stresses exceeding 40 MPa were computed for the southern Dinarides and their foreland with a maximum of 70 MPa at a kink of the Dinaric suture. Although this local maximum may be caused by an artificial corner effect, according to calculations of seismic energy release by Gerner *et al.* (1999) this area is in fact most tectonically active in Europe. In contrast to this seismically active realm, the southern part of the Adria block, where stresses are also very high, is lacking intensive seismicity. In this case, large tectonic stresses are not discharged within the cold and rigid indenter, but instead are efficiently transmitted to surrounding areas (Anderson & Jackson 1987). In the centre of the Pannonian region, the Tisza block is characterized by differential stresses in the order of 20–40 MPa, with a tendency to

decrease northeastwards. Stresses drop to approximately 20 MPa in the Alcapa block and to below 10 MPa in the Transylvanian basin. Minimum stress magnitudes, below 10 MPa, are calculated for the Eastern Carpathians and the eastern part of the EEC. The western part of the EEC is exposed to tectonic stresses in the range of 10–20 MPa. In the Palaeozoic platform differential stresses are in the range of 10–30 MPa, depending on the thickness of the lithosphere. Only in the Alpine foreland stresses may rise locally up to 40 MPa. In the Tauern Window high stress anisotropy is produced by orogen-parallel stretching in W–E direction (see Fig. 8).

6.4 Friction coefficients and displacements on faults

In the presented 2-D model, an analysis of fault friction has substantial limitations because a 3-D fault geometry is not included. Our plane strain model implies only purely strike-slip fault displacement. Therefore, the used friction coefficient is an equivalent to that required for the vertical fault plain, and therefore can be named apparent friction coefficient (μ_A). Because vertical faults have a preferential geometry for strike-slip reactivation, apparent friction coefficient represents maximum value, in comparison to coefficient for more realistic fault's geometry. From the numerical experiments a general relationship can be derived: an increase of compression at the boundary, the addition of topography-related stresses and stiffening of the model material make the model tighter, which implies that faults become less mobile.

First we investigated the minimum μ_A values that required to prevent fault motion at a given stress level. In the relatively tight model Mod2 (Table 3) μ_A values in the range of 0.4–0.6 were sufficient to lock almost all faults. Only the Dinaric suture needed $\mu_A = 1$. By comparison with the models having active faults under similar boundary loads (Mod2 and Mod4), it may be shown that the best fit of model is obtained for friction coefficients of active faults less than half of those required to lock the faults. In the relatively tight model Mod4, unrealistically low μ_A values were obtained, namely 0.2–0.3 for the North European plate, 0.1–0.2 for the South European plate and 0.4 for the Dinaric suture. In loose models similar fault motion can be achieved by using higher coefficients. For example, in the preferred model Mod7 friction coefficients increase to 0.4–0.7 for the north European plate, 0.15–0.25 for the South European plate and 0.55 for the Dinaric suture (Fig. 12).

A relatively high value of friction at the Dinaric suture is necessary to transmit sufficient stresses to the Pannonian basin. With low-level friction, the energy of Adria push propagates through the Alps to Western Europe instead of being transmitted across the suture into the Pannonian realm. In turn, an extremely low μ_A is necessary to move the Mur-Žilina fault, which modifies stress directions in the Western Carpathians, according to the concept of stress partitioning between the Bruno-Vistulicum and the Alcapa (Jarosiński 1998). A higher μ_A was postulated for the Małopolska segment of the Carpathian suture (Jarosiński 2005a), which also corresponds with the results of our modelling. Also low μ_A values for other faults in the Pannonian region permits S_H to rotate in the preferred direction. Systematically lower μ_A in the Pannonian region than in the North European plate can be explained by taking into account the origin of fault zones. The Mur-Žilina, mid-Hungarian and Drava faults are young sutures between terranes, accreted to the North European plate in the Neogene (Fodor *et al.* 1999). Since then they underwent numerous strike-slip reactivations. Fractures in the North European plate were active in the Variscan times, later on they underwent only minor reactivation (except the younger Rhine graben). These ancient

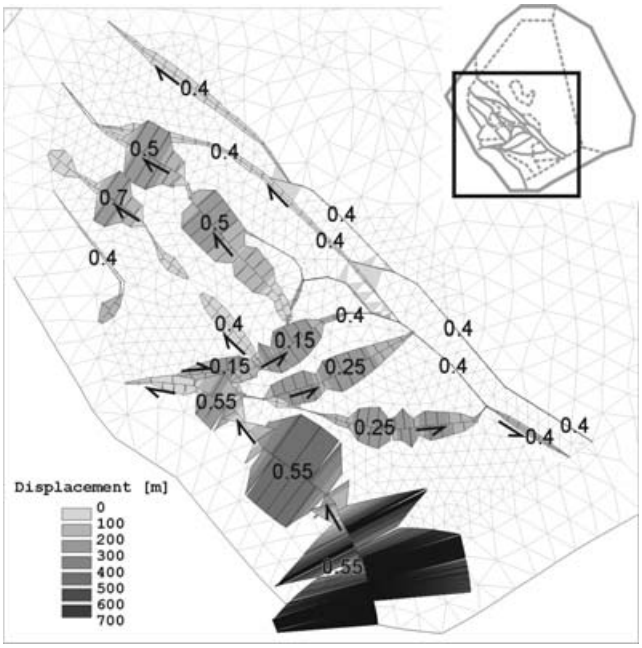

Figure 12. Displacements of faults and preferred values of apparent friction coefficients for the Mod7. Arrows point to the sense of fault offset.

fault zones are probably more intensively healed than the young ones. A higher μ_A of the Dinaric suture can arise from its gentle dip, because this geometry is not prone to strike-slip reactivation.

The calculated fault displacements are compensated by purely elastic deformation, which does not represent true displacements, accumulated over geological time. In Mod7, the largest fault displacements are in the range of 200–500 m, and are calculated for the Dinaric suture, with the exception of the Periadriatic segment, which has less than 100 m of offset (Fig. 11). Intermediate displacements in the range of 100–200 m are evaluated for the Pannonian region. In spite of the relatively high friction coefficients at the Hamburg-Elbe and Franconian lines ($\mu_A >= 0.5$) these faults reveal displacements in the order of 200–300 m. These offsets seem to be too much, as these structures do not reveal significant seismicity. This result suggests that either the geometry of these fault zones is too simple or that these faults are almost completely healed. For the TESZ , our model predicted minor strike-slip reactivation in the range of several tens of metres, which is acceptable proxy, taking into account minor neotectonic and seismic activity of this zone (Guterch & Lewandowska-Marciniak 1975; Gibowicz *et al.* 1981). Both the model and the data indicate that the TTZ stays inactive except for its northernmost branch with the STZ that accommodates minor dextral displacement (Wahlstrom & Grunthal 1994).

7 CONCLUSIONS

The complex stress field in Central Europe can be explained by structural model that incorporates external tectonic forces combined with topography-induced stresses. A satisfactory solution of the model is constrained by stress directions and stress regimes data supplemented by fault reactivation compatibility. We found this composite model to be sensitive to relative changes in loading between the segments of the model boundaries in the range of $0.2^{*}10^{12}$ N m^{-1}. Although the absolute values of the calculated tectonic forces depend on a proper estimation of topographic stresses, differences

between the boundary loads remain relatively stable for a wide range of model solutions.

Our results show that active tectonic zones play a prominent role in generating second-order stress features in the southern part of the European plate. They allow for abrupt changes of stress orientations and regimes between tectonic blocks. Of special importance are the shape and the friction coefficient of the Dinaric suture, which control the effectiveness of stress propagation from the Adria indenter into Central Europe. Topography-related stresses are most important for the calibration of the boundary forces by equilibration of stress regimes in the high mountain ranges like the Alps, the Eastern Carpathians and Scandinavian Mts. Stiffness contrasts between tectonic blocks have only a minor effect on the stress pattern as long as they vary by less than one order of the magnitude. Higher stiffness contrasts impede proper model solution in the vicinity of Pannonian region.

One of the main outcomes of this modelling is the differentiation of tectonic push within the collision zone of Africa and Arabia with Eurasia. Collision-related stresses are transmitted into the interior of Central Europe through the Ionian Sea side of Adria. The tectonic push at this segment is four times stronger than at any other segment of the examined part of collision zone. This suggests a strong mechanical coupling between the Adria indenter and Africa. The counter-clockwise rotation of Adria is forced by the eccentricity between the northward push in the Ionian Sea and the resistance to this push in the Alps. In this case, contribution of the Apennine segment can be neglected. The predicted major pull at the Greek and Aegean segments points out that the Hellenic slab retreat is a likely reason for extension in the Aegean–Balkan region. The Black Sea compression is oblique to the Pontides, probably due to resistive dextral movement along the North Anatolian fault. The eastward decrease in magnitude of the compression indicates that the Arabian push is not effectively transmitted into the EEC across the eastern Black Sea and the Caucasus segments. The ridge push on the NW passive margin of Europe decreases from the North Sea towards the Norwegian Sea, with a rapid drop in between these two segments. This trend reverses at the Arctic Ocean where the ridge push increases in respect to the Norwegian Sea.

Results of the modelling do not support the mechanism of transmission of intraplate stresses from Western Europe through the Bohemian massif into the Pannonian region. Furthermore, a tectonic push or pull from the Vrancea zone is not strictly required to successfully predict the stress pattern in Central Europe and, more particularly, in the Pannonian region. Incompatibility of the modelled stress direction with data points to two factors missing in our 2-D approach. One is the plate flexure due to post-glacial uplift of Fennoscandia and the second suspected factor could be mantle plume below the Eger graben. We also propose that the recent extension or eastward escape of the Tauern Window originates mainly from the tectonic push of the Adria indenter and not from topography-induced collapse. Movement of tectonic blocks in the Pannonian region produces the general pattern of eastward escape in front of the obliquely advancing Adria indenter, which is probably enhanced by slab retreat suction from the Aegean region.

ACKNOWLEDGMENTS

Colleagues from the Polish Geological Institute, Ola Polechońska and Stanisław Wybraniec are thanked for providing unpublished geophysical data that improved the construction of the model. Ewa Szynkaruk and Wojtas Nowikowski are thanked for careful reading and correction of the manuscript. This research was supported by the Netherlands Research Centre for Integrated Solid Earth Science (ISES) and the Polish Geological Institute project no. 6.20.9214.00.0.

REFERENCES

Aleksandrowski, P., 1995. The significance of major strike-slip displacements in the development of the Variscan suture of the Sudetes (SW Poland) (In Polish with English abstract), *Przegląd Geologiczny,* **43,** 745–754.

Altiner, Y., 2001. The contribution of GPS data to the detection of the Earth's crust deformations illustrated by GPS campaigns in the Adria region, *Geophys. J. Int.,* **145,** 550–559.

Anderson, H. & Jackson, J., 1987. Active tectonics of the Adriatic regions, *Geophys. J. R. astr. Soc.,* **91,** 937–983.

Andeweg, B., 2002. Cenozoic tectonic evolution of the Iberian Peninsula: causes and effects of changing stress fields, Netherlands Research School of Sedimentary Geology publication 20020101, Amsterdam, 1–178.

Ansorge, J., Blundell, D. & Meller, St., 1992. Europe's lithosphere – seismic structure, In: *A Continent Revealed - The European Geotravers*, pp. 33–69, eds, Blundell, D., Freeman, R. & Mueller, S., Cambridge University Press, Cambridge.

Aric, K., 1981. Deutung krustenseismischer und seismologisher Ergebnisse in Zusammenhänge mit der Tektonik des Alpenostrandes. Aus den Sitzungsberichten der Öesterr, *Acad. Wiss. Mathem. Naturw. Kl., Wien*, **190**(8–10), 235–312.

Arthaud, F. & Matte, P., 1977. Late Paleozoic strike-slip faulting in southern Europe and northern Africa: Result of a right-lateral shear zone between the Appalachians and the Urals, *Geol. Soc. Amer. Bull*., **88**, 1305–1320.

Bada, G., 1999. Cenozoic stress field evolution in the Pannonian Basin and surrounding orogens, Netherlands Research School of Sedimentary Geology, Amsterdam, publication 990101, 1–204.

Bada, G., Cloetingh, S., Gerner, P. & Horváth, F., 1998. Sources of recent tectonic stress in the Pannonian region: inferences from finite element modeling, *Geophys. J. Int.,* **134,** 87–101.

Bada, G., Horváth, F., Cloetingh, S., Coblentz, D. & Tóth, T., 2001. Role of topography-induced gravitational stresses in basin inversion: the case study of the Pannonian basin, *Tectonics*, **20**(3), 343–363.

Balla, Z., 1988. On the origin of structural pattern of Hungary, *Acta. GEol. Hung.*, **31,** 53–63.

Balling, N., 1995. Heat flow and thermal structure of the lithosphere across the Baltic Shield and northern Tornquist Zone, *Tectonophysics*, **244,** 13–50.

Bankwitz, P., Schneider, G., Kämpf, H. & Bankwitz, E., 2003. Structural characteristic of epicentral areas in Central Europe: study case Cheb Basin (Czech Republic), *J. Geodynamics,* **35**(1–2), 5–32.

Becker, A., Blümling, P. & Müller, W.H., 1987. Recent stress field and neotectonics in the Eastern Jura Mountains, Switzerland, *Tectonophysics,* **135,** 277–288.

Berthelsen, A., 1992. Mobile Europe, in *A Continent Revealed—The European Geotravers,* pp. 11–32, eds Blundell, D., Freeman, R. & Mueller, S., Cambridge University Press, Cambridge.

Brereton, R. & Mueller, B., 1991. European stress: contribution from borehole breakouts, in *Tectonic stress in the lithosphere,* pp. 165–179, eds Whitmarsh, R.B., Bott, M.H.P., Fairhead, J.D. & Kusznir N.J., The Royal Society, London.

Carminati, E., Wortel, M.J.R., Meijer, P.Th. & Sabadini, R., 1998. The two-stage opening of the western-central Mediterranean basin: a forward modeling test to a new evolutionary model, *Earth planet. Sci. Lett.,* **160,** 667–679.

Champagnac, J.-D., Sue, C., Delacou, B. & Burkhard M., 2004. Brittle deformation in the inner NW Alps: from early orogen-parallel extrusion to late orogen-perpendicular collapse, *TerraNova*, **16,** 368–370.

Channell, J.E.T., D'Argenio, B. & Horváth, F., 1979. Adria, the African Promontory in Mesozoic Mediterranean paleogeography, *Earth Science Reviews,* **15,** 213–292.

Chiarabba, C., Jovane, L. & DiStefano, R., 2005. A new view of Italian seismicity using 20 years of instrumental recordings, *Tectonophysics*, **395,** 251–268.

Cloetingh, S.A.P.L., Wortel, M.J.R. & Vlaar, N.J., 1982. Evolution of passive continental margins and initiation of subduction zones, *Nature,* **297,** 139–142.

Cloetingh, S. & Banda, E., 1992. Europe's lithosphere—physical properties. Mechanical structure, in *A Continent Revealed—The European Geotraverse,* pp. 80–91, eds Blundell, D., Freeman, R. & Mueller, S., Cambridge University Press, Cambridge.

Cloetingh, S., Spadini, G., Van Wees, J.D. & Beekman, F., 2003. Thermo-mechanical modeling of Black Sea Basin (de)formation, *Sedimentary Geology,* **156,** 169–184.

Cloetingh, S., Burov, E., Matenco, L., Toussaint, G., Bertotti, G., Andriessen, P.A.M., Wortel, M.J.R. & Spakman, W., 2004. Thermo-mechanical controls on the mode of continental collision in the SE Carpathians (Romania), *Earth planet. Sci. Lett.*, **218,** 57–76.

Coblentz, D.D., Richardson, R.M. & Sandiford, M., 1994. On the gravitational potential of the Earth's lithosphere, *Tectonics,* **13,** 929–945.

Console, R., Givambattista, R., Favali, P., Presgrave, B.W. & Smriglio, G., 1993. Seismicity of the Adriatic microplate, *Tectonophysics,* **218,** 343–357.

Cook, R.D., Malkus, D.S. & Plesha, M.E., 1989. *Concepts and Applications of Finite Element Analysis,* John Wiley & Sons, New York.

Csontos, L., 1995. Tertiary tectonic evolution of the intra-Carpathian area: a review, *Acta Vulcan.*, **7,** 1–13.

Dart, C.J., Inderhaugh, O.H., Kløvian, O. & Ottesen, C., 1995. The present stress regime in the Barents Sea from borehole breakouts, in: Proceeding of the Workshop '*Rock Stress in the North Sea*', 13–14 February, Trondheim, pp. 179–190.

Dercourt, J. *et al.*, 1986. Geological evolution of the Tethys belt from the Atlantic to the Pamirs since the LIAS, *Tectonophysics*, **123,** 241–315.

Fejerskov, M. & Lindholm, C.D., 2000. Crustal stress in and around Norway: an evaluation of stress-generating mechanisms, in *Dynamics of the Norwegian Continental Margin,* Vol. 167, pp. 451–467, eds Nottevedt, A., Larsen, B.T., Olaussen, S., Torudbakken, B., Skogseid, J., Gabrielsen, R.H., Brekke, H. & Birkeland, O., *Geol. Soc. Spec. Publ.*

Fleitout, L., 1991. The sources of lithospheric tectonic stresses, *Phil. Trans. R. Soc. Lond.,* **337,** 73–81.

Flerit, F., Armijo, R., King, G. & Meyer, B., 2004. The mechanical interaction between the propagating North Anatolian Fault and the back-arc extension in the Aegean. *Earth planet. Sci. Lett.,* **224,** 347–362.

Fodor, L., Csontos, L., Bada, G., Gyfri, I. & Benkovics, L., 1999. Tertiary tectonic evolution of the Pannonian Basin system and neighbouring orogens: a new synthesis of paleostress data, in *The Mediterranean Basin: Tertiary Extension within the Alpine Orogen,* Vol. 156, pp. 295–334, eds Durand, B., Jolivet, L., Horvath, F. & Seranne M., *Geol. Soc. London Spec. Publ.*

Gerner, P., Bada, G., Dövenyi, P., Müller, B., Oncescu, M., Cloetingh, S. & Horváth F., 1999, Recent tectonic stress and crustal deformation in and around the Pannonian Basin: data and models, in *The Mediterranean Basins: Tertiary Extension Within the Alpine Orogen,* Vol. 156, pp. 269–294, eds Durand, B., Jolivet, L., Horváth, F. & Seranne, M., Geological Society, Special Publ.

Gibowicz, S.J., Głazek, J. & Wysokiński, L., 1981. Zjawiska sejsmiczne w rejonie kopalni wêgla brunatnego Bełchatów (English abstract), *Przegląd Geologiczny,* **5,** 246–250.

Gibowicz, S.J., 1984. The mechanism of large mining tremors in Poland, in *Proceedings of the 1st International Congress on Rockburst and Seismicity in Mines,* pp. 17–28, eds Guy, N.C. & Wainwright, E.M., Johannesburg, 1982, SAIMM.

Goes, S., Loohuis, J.J.P., Wortel, M.J.R. & Govers, R., 2000. The effect of plate stress and shallow mantle temperatures on tectonics of northwestern Europe, *Global Planet. Change,* **27,** 23–38.

Gölke, M. & Coblentz, D., 1996. Origins of the European regional stress field, *Tectonophysics,* **266,** 11–24.

Grad, M. *et al.*, 1999. Crustal structure of the Mid-Polish Trough beneath the Teisseyre-Tornquist Zone seismic profile, *Tectonophysics,* **314,** 145–160.

Grenerczy, G., Kenyeres, A. & Fejes, I., 2000. Present crustal movement and strain distribution in Central Europe inferred from GPS measurements, *J. geophys. Res.,* **105**(B9), 21 835–21 846.

Grünthal, G. & Stromeyer, D., 1992. The recent crustal stress field in central Europe: trajectories and finite element modeling, *J. geophys. Res.,* **97,** 11 805–11 820.

Gutdeutsch, P. & Aric, K., 1988. Seismicity and neotectonics of the East Alpine-Carpathian and Pannonian area, *AAPG Memoir,* **45,** 183–194.

Guterch, A. *et al.*, 1994. Crustal structure of the transition zone between Precambrian and Variscan Europe from new seismic data along LT-7 profile (NW Poland and eastern Germany), *C.R. Acad. Sci. Paris,* **319,** 1489–1496.

Guterch, A., Grad, M., Thybo, H., Keller, G.R. & The POLONAISE Working Group, 1999. POLONAISE'97—an international seismic experiment between Precambrian and Variscan Europe in Poland, *Tectonophysics,* **314,** 101–121.

Guterch, A., Grad, M., Špičák, A., Brückl, E., Hegedüs, E., Keller, G.R. & Thybo, H., 2003. An overview of recent seismic refraction experiments in Central Europe, *Studia geophysica et geodaetica,* **47,** 651–657.

Guterch, B. & Lewandowska-Marciniak, H., 1975. Seismicity of Poland (English summary), in *Współczesne i neotektoniczne ruchy skorupy ziemskiej w Polsce T.1,* pp. 29–32, eds Liszkowski, J. & Stochlak, J., Wydawnictwa Geologiczne, Warsaw.

Hatzfeld, D., Besnard, M., Makropoulos, K. & Hatzidimitriou, P., 1993. Microearthquake seismicity and fault plane solutions in the southern Aegean and its tectonic implications, *Geophys. J. Int.,* **115,** 799–818.

Hefty, J., 1998. Estimation of site velocities from CEGRN GPS campaigns refered to CERGOP reference frame, *Publ. Warsaw University of Technology, Institute of Geodesy and Geodetic Astronomy,* **9**(39), 67–79.

Henderson, J., 1991. An estimate of stress tensor in Sweden using earthguake focal mechanisms, *Tectonophysics,* **192,** 231–244.

Horváth, F., 1993. Towards a mechanical model for the formation of the Pannonian Basin, *Tectonophysics*, **226**, 333–357.

Horváth, F., 1995. Phases of compression during the evolution of the Pannonian basin and its bearing on hydrocarbon exploration, *Mar. Pet. Geol.,* **12,** 837–844.

Horváth, F. & Cloetingh, S., 1996. Stress-induced late-stage subsidence anomalies in the Pannonian basin, *Tectonophysics,* **266,** 287–300.

Huber, K. *et al.*, 1997. Analysis of borehole televiewer measurements in the Vorotilov drillhole, Russia—first results, *Tectonophysics,* **275,** 261–272.

Hurtig, E., Čermàk, V., Haenel, R. & Zui, V., 1992. *Geothermal Atlas of Europe,* Verlagsgesellschaft, Gotha.

Jackson, J.A. & McKenzie, D.P., 1988. The relationship between plate motions and seismic moment tensors, and the rates of active deformation in the Mediterranean and Middle East, *Geophys. J. R. astr. Soc.,* **93,** 45–73.

Jackson, J., Priestley, K., Allen, M. & Berberian, M., 2002. Active tectonics of the South Caspian Basin, *Geophys. J. Int.,* **148,** 214–245.

Jarosiński, M., 1998. Contemporary stress field distortion in the Polish part of the Western Outer Carpathians and their basement, *Tectonophysics,* **297,** 91–119.

Jarosiński, M., 1999. Present-day tectonic stress directions in Poland and their relation to intra-plate motions as determined by mean of GPS, Paper presented at 2nd Euroconference on WSM—Deformation and Stress in the Earth's Crust, Aspo Hard Rock Laboratory, Sweden.

Jarosiński, M., 2001. Present-day geodynamics of Palaeozoic complex beneath the Outer Carpathians based on logs and core analysis in the Tarnawa 1 well (English summary), *Prace Państwowego Instytutu Geologicznego,* **174,** 119–132.

Jarosiński, M., 2005a. Ongoing tectonic reactivation of the Outer Carpathians and its impact on the foreland: results of borehole breakout measurements in Poland, *Tectonophysics,* **410**(1–4), 189–216.

Jarosiński, M., 2005b. Recent tectonic stress regime in Poland based on analyses of hydraulic fracturing of borehole walls (English abstract), *Przegląd Geologiczny,* **53,** 863–872.

Jarosiński, M. & Dąbrowski, M., 2006. Rheological models of the lithosphere across the Trans-European Suture Zone in northern and western part of Poland (English summary). *Prace PIG,* in press.

Jarosiński, M., Poprawa, P. & Beekman, F., 2002. Rheological model of the lithosphere across TESZ: LT-7 DSS profile in NE Poland (English abstract), *Przegląd Geologiczny,* **50,** 1073–1081.

Jensen, S.L., Janik, T., Thybo, H. & The POLONAISE Working Group, 1999. Seismic structure of the Palaeozoic Platform along POLNAISE'97 profile P1 in northwestern Poland, *Tectonophysics,* **314,** 123–143.

Jolivet, L., 2001. A comparison of geodetic and finite strain in the Aegean, geodynamic implications, *Earth planet. Sci. Lett.,* **187,** 95–104.

Jones, C.H., Unruh, J.R. & Sonder, L.J., 1996. The role of gravitational potential energy in active deformation in the southwestern United States, *Nature,* **381,** 37–41.

Kahle, H-G., Cocard, M., Peter, Y., Geiger, A., Reilinger, R., Barka, A. & Veis, G., 2000. GPS-derived strain rate field within the boundary zones of the Eurasian, African, and Arabian Plates, *J. geophys. Res.,* **105**(B10), 23 353–23 370.

Kotzev, V., Nakov, R., Burchfiel, B.C., King, R. & Reilinger, R., 2001. GPS study of active tectonics in Bulgaria: results from 1996–1998, *J. Geodyn.,* **31**(2), 189–200.

Królikowski, C. & Petecki, Z., 1997. Crustal structure at the Trans-European Suture Zone in northwest Poland based on gravity data, *Geol. Mag.,* **134**(5), 661–667.

Lankreijer, A., Bielik, M., Cloetingh, S. & Majcin, D., 1999. Rheology predictions across the western Carpathians, Bohemian massif, and Pannonian basin: implications for tectonic scenarios, *Tectonics,* **18,** 1139–1153.

Lillie, J.R., Bielik, M., Babuska, V. & Plomerová, J., 1994. Gravity modelling of the Lithosphere in the Eastern Alpine–Western Carpathian–Pannonian Basin Region, *Tectonophysics,* **231,** 215–235.

Liunggren, C., 1992. Regional patterns of tectonic stress in Europe, *J. geophys. Res.,* **97**(B8), 11 783–11 803.

Locardi, E., 1988. The origin of the Apenninic arcs, *Tectonophysics,* **146,** 105–123.

Majorowicz, J. & Plewa, S., 1979. Study of heat flow in Poland with special regard to tectonophysical problems, in *Terrestial Heat Flow in Europe,* pp. 240–251, eds Čermak V. & Rybach L., Springer-Verlag, Berlin.

Mantovani, E., Babbuci, D., Albarello, D. & Mucciarelli, M., 1990. Deformation pattern in the central Mediterranean and behaviour of the African/Adriatic promontory, *Tectonophysics,* **179,** 63–79.

Mantovani, E., Viti, M., Alberto, D., Tamburelli, C., Babbucci, D. & Cenni, N., 2000. Role of kinematically induced horizontal forces in Mediterranean tectonics: insights from numerical modelling, *J. Geodyn.,* **30,** 287–320.

Marotta, A.M., Bayer, U., Thybo, H. & Scheck, M., 2002. Origin of the regional stress in the North German basin: results from numerical modelling, *Tectonophysics,* **360,** 245–264.

Martin, M., Lorenz, F.P., Onescu, M.C. & Wenzel, F., 1998. Joint tomography inversion of the Carpathian arc in Romania, *Ann. Geophys.,* **16**(I), C111.

Márton, E. & Fodor, L., 1995. Combination of paleomagnetic and stress data: a case study from North Hungary, *Tectonophysics,* **242,** 99–114.

Matenco, L., Zoetemeijer, R., Cloetingh, S. & Dinu, C., 1997. Lateral variations in mechanical properties of the Romanian external Carpathians: inferences of flexure and gravity modelling, *Tectonophysics,* **282,** 147–166.

Matte, P., 1991. Accretionary history and crustal evolution of the Variscan Belt In Western Europe, *Tectonophysics,* **196,** 309–337.

McClusky, S. *et al.*, 2000. Global Positioning System constraints on plate kinematics and dynamics in the eastern Mediterranean and Caucasus, *J. geophys. Res.,* **105,** 5695–5719.

Meijer, P.Th. & Wortel, M.J.R., 1997. Present-day dynamics of the Aegean region: a model analysis of the horizontal pattern of stress and deformation, *Tectonics,* **16,** 879–895.

Milne, G.A., Davis, J.L., Mitrovica, J.X., Scherneck, H.-G., Johansson, J.M., Vermeer, M. & Koivula, H., 2001. Space-Geodetic Constraints on Glacial Isostatic Adjustment in Fennoscandia, *Science,* **291,** 2381–2385.

Minster, J.B. & Jordan, T.H., 1978. Present-day plate motions, *J. geophys. Res*., **83**, 5331–5375.

Müller, B., Zoback, M.L., Fuchs, K., Mastin, L. Gregersen, S., Pavoni, N., Stephansson, O. & Liunggren, C., 1992. Regional patterns of tectonic stress in Europe, *J. geophys. Res.,* **97**(B8), 11 783–11 803.

Müller, B., Wehrle, V., Zeyen, H. & Fuchs, K., 1997. Short-scale variations of tectonic regimes in the western European stress province north of the Alps and Pyrenees, *Tectonophysics,* **275,** 199–219.

Nemcok, M., Pospisil, L., Lexa, J. & Donelick, R.A., 1998. Tertiary subduction and slab break-off model of the Carpathian–Pannonian region, *Tectonophysics,* **295,** 307–340.

Oncescu, M.C., 1987. On the stress tensor in Vrancea region, *J. Geophys.,* **62,** 62–65.

Pan, M., Sjöberg, L.E. & Talbot, C.L., 2001. Crustal movements in Skåne, Sweden, between 1992 and 1998, *J. Geodyn.,* **31,** 311–322.

Panza, G.F., 1985. Lateral variations in the lithosphere in correspondence of the Southern segment of EGT, in *Second EGT Workshop: The Southern Segment,* pp. 47–51, eds Galson, D.A. & Muller, St., European Science Foundation, Strasbourg, France.

Pascal, C., Roberts, D. & Gabrielsen, R.H., 2005. Quantification of neotectonic stress orientations and magnitudes from field observations in Finnmark, northern Norway, *J. Struct. Geol.,* **27,** 859–870.

Pasquale, V., Verdoya, M. & Chiozzi, P., 1991. Lithospheric thermal structure in the Baltic shield, *Geophys. J. Int.,* **106,** 611–620.

Peresson, H. & Decker, K., 1997. The Tertiary dynamics of the nothren Eastern Alps (Austria): changing paleostress in a collisional plate boundary, *Tectonophysics,* **272,** 125–157.

Picha, F.J., 2002. Late orogenic strike-slip faulting and escape tectonics in frontal Dinarides-Hellenides, Croatia, Yugoslavia, Albania, and Greece, *AAPG Bull*., **86**, 1659–1671.

Plenefisch, T. & Bonjer, K.-P., 1997. The stress field in the Rhine Graben area inferred from earthquake focal mechanisms and estimation of frictional parameters, *Tectonophysics,* **275,** 71–97.

Radulian, M., Mândrescu, N., Panza, G.F., Popescu, E. & Utale, A., 2000. Characterization of seismogenic zones in Romania, *Pure appl. Geophys.,* **157,** 57–77.

Ranalli G., 1995. Rheology of the Earth, Chapman and Hall, London, 413.

Reilinger, R.E. *et al.*, 1997. Global Positioning System measurements of present-day crustal movements in the Arabia-Africa-Eurasiaplate collision zone, *J. geophys. Res.,* **102,** 9983–9999.

Reinecker, J., Heidbach, O. & Mueller, B., 2003. The 2003 release of the World Stress Map (available online at www.world-stress-map.org).

Reinecker, J. & Lenhardt, W.A., 1999. Present-day stress field and deformation in eastern Austria, *Int. J. Earth Sci.,* **88,** 532–550.

Rosenbaum, G. & Lister, G.S., 2004. Neogene and Quaternary rollback evolution of the Tyrrhenian Sea, the Apennines, and the Sicilian Maghrebides, *Tectonics,* **23,** 1013–1029.

Roth, E. & Fleckenstein, P., 2001. Stress orientations found in north-east Germany differ from the West European trend, *TerraNova,* **13,** 289–296.

Selverstone, J., 2005. Are the Alps collapsing? *Annu. Rev. Earth planet. Sci.* **33,** 113–132.

Špičák, A., Horálek, J., Boušková, A., Tomek, Č. & Vank, J., 1999. Magma intrusions and earthquake swarm occurrence in the western part of the Bohemian Massif, *Studia Geophysica et Geodaetica,* **43,** 87–106.

Stephansson, O., Ljunggren, C. & Jing, L., 1991. Stress measurements and tectonic implications for Fennoscandia, *Tectonophysics,* **189,** 317–322.

Tari, V., 2002. Evolution of the northern and western Dinarides: a tectonostratigraphic approach, in *Stephan Mueller Special Publication Series 1,* pp. 223–236, eds Bertotti, G., Schulmann, K. & Cloetingh, S.A.P.L., Amsterdam.

Turcotte, D. & Schubert, G., 1982. *Geodynamics: Applications of Continuum Physics to Geological Problems,* John Wiley and Sons, New York, p. 450.

van Mierlo, J., Oppen, S. & Vogel, M., 1997. Monitoring of recent crustal movements in the Eastern Alps with the Global Positioning System (GPS), *Tectonophysics,* **275,** 273–283.

Viti, M., Albarello, D. & Mantovani, M., 1997. Rheological profiles in the central-eastern Mediterranean, *Annali di Geofisica,* **40**(4), 849–864.

Wahlstrom, R. & Grunthal, G., 1994. Seismicity and seismotectonic implications in the southern Baltic Sea area, *TerraNova,* **6,** 149–157.

Ward, S.N., 1994. Constraints on seismotectonics of the central Mediterranean from very long baseline interferometry, *Geophys. J. Int.,* **117,** 441–452.

Windhoffer, G., Bada, G., Horváth, F., Cloetingh, S., Szafián, P. & Timár, G., 2003. Pull-apart basin evolution and fault reactivation: a case study of the Derecske trough, Pannonian basin, *Geophys. Res. Abstr.,* **5,** 04140.

Wortel, M.J.R. & Spakman, W., 2000. Subduction and Slab Detachment in the Mediterranean-Carpathian Region, *Science,* **290,** 1910–1917.

Ziegler, P., 1982. *Geological Atlas of Western and Central Europe,* Shell Internationale Petroleum Maatschappij B.V., p. 130.

Ziegler, P.A. & Cloetingh, S.A.P.L., 2004. Dynamic processes controlling evolution of rifted basins, *Earth Sciences Reviews,* **64,** 1–50.